Spring 2019

# An electrical matlab model of plasma electrolytic oxidation

Huize Xue
*New Jersey Institute of Technology*

# Copyright Warning & Restrictions

The copyright law of the United States (Title 17, United States Code) governs the making of photocopies or other reproductions of copyrighted material.

Under certain conditions specified in the law, libraries and archives are authorized to furnish a photocopy or other reproduction. One of these specified conditions is that the photocopy or reproduction is not to be "used for any purpose other than private study, scholarship, or research." If a, user makes a request for, or later uses, a photocopy or reproduction for purposes in excess of "fair use" that user may be liable for copyright infringement,

This institution reserves the right to refuse to accept a copying order if, in its judgment, fulfillment of the order would involve violation of copyright law.

Please Note: The author retains the copyright while the New Jersey Institute of Technology reserves the right to distribute this thesis or dissertation

Printing note: If you do not wish to print this page, then select "Pages from: first page # to: last page #" on the print dialog screen

## ABSTRACT

## AN ELECTRICAL MATLAB MODEL OF PLASMA ELECTROLYTIC OXIDATION

**by**
**Huize Xue**

Plasma Electrolytic Oxidation (PEO), a part of Plasma electrolytic Deposition (PED), has been developing for surface modification of metallic materials in the past 20 years. During PEO process, sample always connect with anode of DC power source, under high temperature, accelerating process of oxidation reaction to from an average and dense oxidation film. A general passage, *Plasma electrolysis for surface engineering*, written by A.L. Yerokhin, X. Nie gives us a trend of what happened during PEO process but did not determine specific material and value. Linxin Zhu's *Development of PEO* invent a new boiling system and investigated relationship between surface roughness and coating and mentioned investigating on resistance of DC current at future work.

In this passage, focusing on the electrical model, PEO process is studied in both experimental and theoretic aspect. In practice, PEO industries could be distinguished by what terms it entered in according to different demand. And, the resistance in this term are quite different because of different structures at surface of sample. Theoretically, three types of electrical models have been built by MATLAB after analyzing the main influence factors of PEO process, which could help us explain how the structure and resistance change.

Experimentally, a Ti-6Al-4V piece was used as a sample to do all PEO experiments. Diversity results was obtained by change the conductivity of electrolyte and applied voltage. Others experimental parameters were controlled to be same as possible like surface roughness, contents of liquid solution and voltage increase speed. All the thing above purpose to make electrical model more reasonable and trustable.

All the experiments were recorded by a camera then select pictures in every second. Then input the statistics in the matrix in MATLAB as the original reference, which is used to compare to the simulation result. So that the simulation model could be adjusted until it meets the experiment results. Thus, the main factors which influence resistance could be inferred.

After analyzing, we found, at passive film stage, the majors resistance consists of resistance of electrolyte and passive oxidation film of anode (Ti-6Al-4V sample). Temperature would slightly influence resistance if electrolyte conductivity is big enough. The U-I in this stage is nearly a straight line. While, at the new oxidation film stage, current is significant increase because gradually dissolve of the passive oxidation film with time. So, the U-I curve is a trend of sharp increase. At the arcing stage, current decrease is because new oxidation film formed, and rest of the resistance is determined by temperature.

Besides, these PEO in three stage was simulated by MATLAB models according to the majority factors analyzed. The simulation results suitable for all kind of PEO in Ti-6Al-4V process with different conductivity but changeless surface roughness and increasing applied voltage. Prediction of optimizing applied voltage is possible with this model in PEO process in Ti-6Al-4V.

# AN ELECTRICAL MATLAB MODEL OF PLASMA ELECTROLYTIC OXIDATION

**by**
**Huize Xue**

**A Master Thesis**
**Submitted to the Faculty of**
**New Jersey Institute of Technology**
**in Partial Fulfillment of the Requirements for the Degree of**
**Master in Material Science and Engineering**

**Interdisciplinary Program in Materials Science and Engineering**

**May 2019**

**APPROVAL PAGE**

**AN ELECTRICAL MATLAB MODEL OF PLASMA ELECTROLYTIC OXIDATION**

**Huize Xue**

| | |
|---|---|
| Dr. Roumiana S. Petrova, Thesis Co-Advisor<br>Senior University Lecturer of Chemistry and Environmental Science, NJIT | Date |
| Dr. Levy, Roland A., Thesis Co-Advisor<br>Distinguished Professor of Physics, NJIT | Date |
| Dr. Tao Zhou, Committee Member<br>Associate Professors of Physics, NJIT | Date |
| Dr. Edgardo Farinas, Committee Member<br>Associate Professors of Chemistry and Environmental Science, NJIT | Date |

## BIOGRAPHICAL SKETCH

**Author:** Huize Xue

**Degree:** Master of Science

**Date:** May 2019

**Undergraduate and Graduate Education:**

- Master of Science in Material Science and Engineering,
  New Jersey Institute of Technology, Newark, NJ 2017

- Bachelor of Engineering in Material Science and Engineering,
  Shenyang University of Technology, Shenyang, P. R. China, 2013

**Major:** Material Science and Engineering

For those I loved, for those who loved me
为了我爱的人，为了爱我的人

## ACKNOWLEDGMENT

I am more than gratefully to appreciate Dr. Roumiana S. Petrova, for all her support and kindness. She is mindful and helpful in research. After a research under her guidance for a year, what I acquired is not only the knowledge but also wisdom in academic.

My special thanks go to Dr. Roland Levy and Dr. Tao Zhou for join my defense committee, for their support and precious time.

Other thanks go to Zhengrong Guo, who pay lots of efforts on helping to deal with statistics in this passage and her support in my daily life.

I am more than appreciated to my senior in laboratory, Linxin Zhu, for all his teaching, guidance and support. He is more than a PhD student, but a role model for me.

At last, thanks NJIT giving me a platform to let me study and improving contentiously.

## TABLE OF CONTENTS

**Chapter** **Page**

**TABLE OF CONTENTS**
(continued)

**Chapter** **Page**

## LIST OF TABLES

**Table** **Page**

## LIST OF FIGURES

**Figure** **Page**

## LIST OF FIGURES
(Continued)

**Figure** **Page**

# CHAPTER 1

# INTRODUCTION

## 1.1 Overview of Plasma Electrolytic Deposition (PED)

Plasma Electro Deposition is a new surface modification technology. Ultra-fast nitriding, carburizing, boriding and oxidation. This technique is carried out in a vacuum chamber. The gas source is carried by an inert gas stream, which is produced by different methods, such as glow discharge, dielectrically barrier discharge, corona discharge, and the like. The electrons in the molecule are excited into free electrons. The remaining molecules carry a positive charge called a cation. As sustained energy is activated, more and more electrons are released and move with high kinetic energy. These electrons collide with cations and molecules to excite more electrons, creating new cations. The accumulation of free electrons in the plasma is called "electronic avalanche" [3]. The cation contains sufficiently high kinetic energy to sputter the matrix atoms and achieve a better diffusion rate due to the high reaction temperature. For example, plasma enhanced CVD utilizes a plasma source to achieve better film deposition efficiency [4-6].

## 1.2 History of Plasma Electrolytic Deposition (PED)

Electrolysis-related discharge phenomena were discovered by Sluginov [1] more than a century ago and were studied in detail by Gunterschultze and Betz in the 1930s [2], and their actual benefits were only used in the 1960s, when McNiell And Gruss used spark discharge to deposit cadmium electrolytes [3,4]. In the 1970s, Markov and colleagues also developed and studied oxide

deposition on aluminum anodes under arcing conditions [5,6]. This technique was later improved and was called (obviously misleading) "micro-arc oxidation" [7]. In the 1980s, the possibility of using surface discharges in oxide deposition on various metals was studied. Snezhko and colleagues [8,9], Markov and colleagues [14-16], Fyedorov et al. This possibility is studied in detail. [17], Gordienko and colleagues [18-20] and Germany Kurze and colleagues [21-24], which

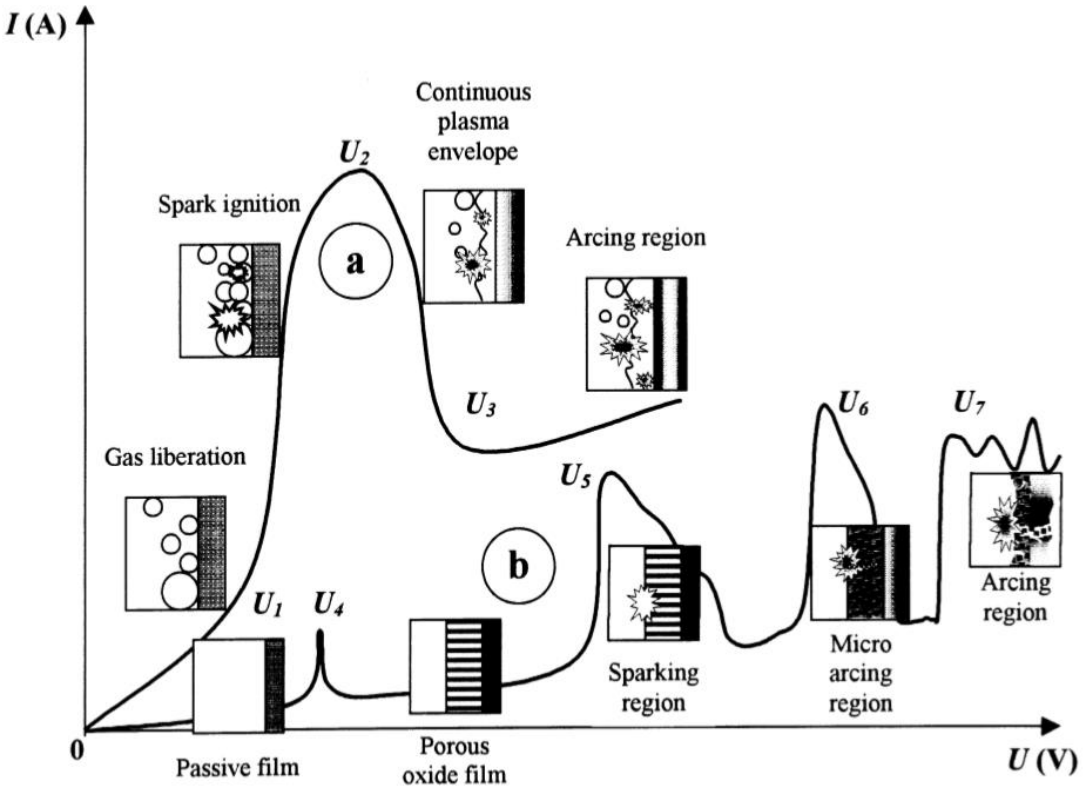


**Figure 2.1.1** Two kinds of current–voltage diagram for the processes of plasma electrolysis: discharge phenomena are developed (a) in the near-electrode area and (b) in the dielectrical film on the electrode surface.

Source: A.L. Yerokhin, X. Nie, A. Leyland, A. Matthews, S.J. Dowey. Plasma electrolysis for surface engineering. Surface and Coating Technology 122 (1999) 73-93.

introduced early industrial applications [25-29]. Researchers in the United States and China are also involved in this field [30-33]. Due to the relatively sparse information about process phenomenology, sometimes lack of understanding, different (and not always physically correct)

terms have been used in most of the above studies, essentially the same technique: 'Microplasma oxidation ', 'Anode spark electrolysis', 'Plasma electrolytic anode treatment', 'Anodischen oxidation under Funkenentladung' (anod oxidation under spark discharge), is a typical example of a common description of 'plasma electrolytic oxidation' (PEO).

Parallel to these developments, Lazarenko and colleagues [34-36] observed the heating effect of surface discharges in liquid electrolytes and used them for metal heat treatment purposes. This technique is referred to as "electrolytic plasma heating." In addition, Duradzhy and colleagues studied the effects of thermal deformation during plasma electrothermal heating [37-39], which also noted the phenomenon of electrolyte elements dispersed to the electrode surface. In the 1980s, these effects were used to develop a process for surface saturation of bulk materials with various alloying elements [39, 40]; therefore, an industry called "plasma electrolyte saturation" (PES) emerged. New possibilities for application. However, in order to exploit its potential in a wider range of surface engineering applications, further developments in plasma electrolysis processes require a better understanding of the physical and chemical background of the plasma phenomena occurring on the electrodes during electrolysis. To emphasize the common principles of the plasma electrolysis process described above, the general term plasma electrolytic deposition (PED) is used herein to include a set of techniques commonly under the headings of PEO and PES [41-43].

### 1.3 Application of PED

Ti and Ti alloys have good mechanical properties, corrosion resistance and biocompatibility, making them a matrix material for bioactive implanted PEO research. As mentioned above, more variables in the process need to be considered, and for industrial scale, the process should be more

controllable. For example, we have found that surface morphology is highly dependent on processing parameters that have not yet received attention.

As with the PEO oxidation process, scientists have also achieved the achievement of HA deposition on Ti-6Al-4V or pure Ti to improve biocompatibility. However, the process parameters of the treatment are different in the paper, and the explanation of the reaction is not given in detail. In our experiments, more variables should be developed to better control treatment. In addition, in previous studies, PES studied carburizing, nitriding, but not boronization. Boronization on ferrous steel provides a hard coat of up to 1700 HV compared to nitriding 800 HV and carburizing 600 HV. High hardness results in high wear resistance while maintaining the same corrosion resistance. Boride is also a self-lubricating material [21-23]. To date, the boronization technique has two preferred directions, conventional plasma (CVD) and paste boronization. The development of electrolytic plasma boronization is not only due to its high efficiency but also a non-toxic and low-cost boronization process.

### 1.4 Phenomenology and Current-Voltage Characteristics

It is well known that the electrolysis of aqueous solutions is accompanied by a number of electrode processes. In particular, the liberation of gaseous oxygen and/or metal oxidation occurs on the anodic surface. Depending on the electrolyte chemical activity in respect to the metal, the oxidation process can lead either to surface dissolution or to oxide film formation. Liberation of gaseous hydrogen and/or cation reduction can also occur on the cathodic surface.

The above-mentioned processes affect the characteristic current–voltage profile of the electrochemical system. A ‘type-a’ current–voltage plot represents a metal–electrolyte system with

underlying gas liberation on either the anode or cathode surface; ‘type-b’ represents a system where oxide film formation occurs [39,41]. At relatively low voltages the kinetics of the electrode processes for both systems conform to Faraday’s laws and the current–voltage characteristics of the cell vary according to Ohm’s law. Thus, an increase in voltage leads to a proportional rise in the current (region ‘0-U1’ in the type-a system and ‘0-U4’ in the type-b system). However, beyond a certain critical voltage, the behavior of a particular system may change significantly.

For a type-a system in the region U1–U2, a potential rise leads to current oscillation accompanied by luminescence the current rise is limited by a partial shielding action of gaseous reaction products (O2 or H2) over the electrode surface. In areas where the electrode remains in contact with the liquid, however, the current density continues to rise, causing local boiling (ebullition) of the electrolyte adjacent to the electrode. Upon progression to point U2 the electrode is enshrouded by a continuous gaseous vapor plasma envelope of low electricalal conductivity. Almost all of the voltage across the cell is now dropped in this thin, near-electrode region. The electrical field strength E within this region therefore reaches a value between 106 and 108 V/m, which is sufficient for initiation of ionization processes in the vapor envelope. The ionization phenomena appear initially as a rapid sparking in scattered gaseous bubbles and then transform into a uniform glow distributed throughout the vapor plasma envelope. Due to the hydrodynamic stabilization of the vapor envelope in the region U2–U3, the current drops and, beyond point U3, the glow discharge transforms into intensive arcing accompanied by a characteristic low-frequency acoustic emission [44-46].

The behavior of type-b systems is more complicated. Firstly, the passive film previously formed begins to dissolve at point U4, which, in practice, corresponds to the corrosion potential

of the material. Then, in the region of passivation U4–U5 a porous oxide film grows, across which most of the voltage drop now occurs. At point U5, the electrical field strength in the oxide film reaches a critical value beyond which the film is broken through due to impact or tunneling ionization [42,43]. In this case, small luminescent sparks are observed to move rapidly across the surface of the oxide film, facilitating its continued growth. At point U6, the mechanism of impact ionization is supported by the onset of thermal ionization processes and slower, larger arc discharges arise. In the region U6–U7 thermal ionization is partially blocked by negative charge build-up in the bulk of the thickening oxide film, resulting in discharge decay shorting of the substrate. This effect determines the relatively low power and duration of the resultant arc discharges, i.e. micro-discharges, which are (somewhat misleadingly) termed ‘micro arcs’ [7]. Owing to this ‘micro-arcing’, the film is gradually fused and alloyed with elements contained in the electrolyte. Above the point U7, the arc micro-discharges occurring throughout the film penetrate through to the substrate and (since negative charge blocking effects can no longer occur) transform into powerful, arcs, which may cause destructive effects such as thermal cracking of the film.

## 1.5 Method

### 1.5.1 Oxide Coating on Ti by PEO method

In our experiment, the focus is on the new variables involved in the preparation of the samples and the treatment, including the effect of the roughness of sample on ignition voltage, the effect of the roughness of the sample on surface morphology of coating, the effect of the roughness of sample on corrosion resistance. Experiments are designed to give a theoretical explanation why and how the roughness of samples during the sample preparation will affect the process and the properties base on both the testing result and theoretical study. The data of experiment will also be used for research on mechanism explanation of PEO and process modeling. Temperature controlling will be our target since PEO has a great potential to provide oxidation coating on the low melting point metals. Eventually, the electrolyte composition, treatment parameters, and modeling will be applied on Al and Mg Alloy for a universal, controllable process setup for PEO on all low melting temperature valve metal.

### 1.5.2 Matrix Laboratory (MATLAB) Software

MATLAB (matrix laboratory) is a multi-paradigm numerical computing environment and proprietary programming language developed by MathWorks. MATLAB allows matrix manipulations, plotting of functions and data, implementation of algorithms, creation of user interfaces, and interfacing with programs written in other languages, including C, C++, C#, Java, Fortran and Python. In this research, this software was used to build up the electrical model and calculate the simulate current.

## 1.6 Difficulties

To develop a model of PED will be a huge challenge since this technique has just been developed less than 20 years. Most research work and study are focusing on the experiment work, these research focus on the optical or mechanical properties, but few people explore the theory part, how the applied voltage and time could influence current and oxidation layer. Interdisciplinary knowledge is required to explain the mechanism. For example, the electricalal and heat transfer equations help a better understanding of the process before plasma ignition. Thus, in this passage several models were established to investigate the relationship between applied voltage and current and analyzed how the mechanism change under the influence of temperature and phase change.

For developing a simulated model, a large amount of factor should be considered, especially factors influence the resistance such as the temperature, oxidation film and electrolyte concentration. Thus, the simulation must consider electrical field, temperature field and phase field. It is difficult to determine which are major factors and which are minority factors. The former one would influence the current a lot while the other one would have near no influence. Once the factors are wrongly omitted or mis-taken into account, the simulated current would never approximate to the true one.

The resistance of electrolyte is a thorny part to establish a model, since both electrodes were immersed in electrolyte. Although the electrolyte is a cylinder as same as beaker, whether the non-right area should be taken into account. In addition, both ions move model and liner resistance model suit the circuit of electrolyte. Besides, the distribution of different concentration would also a kind of problem.

# CHAPTER 2

# LITERATURE REVIEW

T.H. Teh and A. Berkani [55] use alkaline pyrophosphate/aluminate as an electrolyte to apply PEO on Ti-6Al-4V alloy. The specimens are anodized at a current density of 20 mA/cm2 in an electrolyte consisting of 0.03 M tetra sodium pyrophosphate ($Na_4P_2O_7$ $10H_2O$), 0.0178 M potassium hydroxide (KOH) and 0.06M sodium aluminate ($NaAlO_2$) at 293K and the treatment voltage is at 300V. SEM detects the composition of oxidation coating, EDS and TEM results reveal that thickness of oxidation layer is related to treatment voltage meanwhile initial growth of oxidation layer starts as low as 80V. Towards this article, I decided to use Ti-6Al-4V alloy as the experiment anode and determined the voltage used in the experiment which is 0-200V.

Wenbin Xue, Chao Wang [56] Aqueous solution of 10 g/L NaAlO2 is used as the electrolyte for PEO on Ti-6Al-4V alloy. The structural analysis of oxidation is inspiring that from observation of the previous experiment, usually multiple layers of oxidation coating on the Ti alloy same as the paper described. The difference between general observation and their article is that their observation will be more closed to the multi-layer structure of oxide coating by a conventional anodic process on Ti alloy. There will be two layers of oxide, the inner layer of oxide is a dense, non-porous nano-scale passive layer consist of amorphous Ti oxide. This layer is colorful which related to the thickness of the layer, shown in Figure 2.5. Towards this thesis, we know how is a firmly oxidation layer looks like. Then, we will know when to stop the experiment.

Linxin Zhu [41] is studied in both theoretical and experimental directions. Theoretically, it is for the first time that a “nucleation boiling to film boiling” theory is put forth after investigating the PED technique, by introducing thermodynamics and fluid dynamics. The PED conducted at

different boiling statuses is simulated by a Finite Element Method (FEM), showing different plasma ignition procedures at nucleation boiling and film boiling, respectively. Its boiling stage help this research a lot in divided all PEO process into 3 model.

The purpose of exploring the knowledge in the boiling field is to understand the relation and interaction between all the possible boiling states involved in PED process. Figure 2.1 [24] shows the four boiling stages: convection, nucleation boiling, transition boiling and film boiling. Convection regime is at a temperature range from the ambient temperature to boiling point, ex 100 °C for water, at atmospherically pressure. The heat flux transfers from the heated wall to the surrounding fluid. No phase change occurs during the convection. The nucleation boiling is the most common boiling status we can observe in our daily life. Separated bubbles nucleate and raise towards the lower pressure gradient. The Critical Heat Flux (CHF), is the value that distinguishes nucleation boiling and transition boiling. As shown in the peak in Figure 2.1, before CHF is nucleation boiling and post-CHF regions are transition boiling and film boiling. At transition boiling, due to a significant bubble nucleation rate, gas/bubble clusters start to merge [25]. If the boiling is on a heated surface, a partial area of the surface of the heater is covered by the bubbles and insulated from the water. Due to the low thermal conductivity of the gas, the heat transfer between the wall and liquid is reduced. When the temperature reaches above the minimum film boiling temperature, all the surfaces of the heater will be covered with bubbles, which forms a continuous gaseous layer. This gaseous layer separates the heating surface and the liquid completely while the most heat is transferred by radiation. According to this theory, we could confirm the influence and the transfer of bubbles and how the heat traveled, which is most helpful to build the models.

In study of R. O Hussein, X Nie, D. O Northwood, A Yerokhin and A Matthews [44]. A plasma electrolytic oxidation (PEO) process was used to produce aluminum oxide coating in a pulsed DC energy mode. The effects of process parameters on the behavior of plasma discharge during PEO treatment were investigated by optical emission spectroscopy (OES) in visible and near-ultraviolet bands (NUV) (285-800 nm). The elements present in the plasma are identified. The plasma electron concentration and temperature are determined using the apparent change of the spectral lines and the line intensity ratio, respectively. The different coating morphologies and the compositions of the different coating surface areas are explained in terms of three types of discharges, either at the substrate / coating interface, in the upper layer or in the upper layer of the coating. This passage let me know the three kinds of PEO process in application, so I divided the model in three parts. Besides, the spectrum research helps me to realize the corresponding thickness of oxidation layer with color.

# CHAPTER 3

# EXPERIMENTAL

As discussed in the previous chapter, there are too many papers studying the chemical composition and treatment parameters while we are looking for a break though in a deeper understanding of this process including the mechanism explanation. One of the purposes of this experiment is to achieve an oxidation layer on the Ti-6Al-4V alloy with sufficient thickness and good corrosion resistance. Second, we seek to establish a modeling to simulation the temperature and gaseous layer formation during the process.

Boiling is important to this research because it directly determine 3 different discharge which using their own models. Sustain bubbles produce on the electrodes is equivalent to reduce the effective area and gas envelop formed under increasing current like a capacitor in DC electrical circuit. The boiling stage is directly influence by current since heat comes from Joule heat. But, in terms of phenomenon, is based on the when separate bubbles can be seen on the surface of the specimen and when the oxidation film formed. According to our theory, if the oxidation coat is generated during the nucleation boiling stage, we can observe randomly distributed single spark flashing and belongs to the first model. If the surface of the specimen is covered with bubbles and oxidation generated, it's in transit boiling stage and belongs to the second model. When solution around electrode achieve to film boiling before oxidation coating formed, it is obviously that gas envelop has already existed and which belongs to the third model.

## 3.1 Sample Preparation

Commercial grade Ti-6Al-4V is used for the experiment as anode. Each sample was cut into 13.5mm in length, 32.5mm in length and 2mm thick by techcut 5 cutting machine. A well-cut

graphite plate which size is 72.5*36*3mm in length, width and thickness was always used as the cathode.

To make sure that surface roughness will not influence the results between difference each experiment. All the sample was grinded by #400 grinder paper to eliminate the oxide layer until all the place showed silver metal color by a metprep 3 grinding machine. Then, roughness of the pre-grinded sample is measured by surface profile meter in 0.118μm. Only if samples meet these requirements could be used in the experiment.

### 3.2 Electrolyte Preparation

In this research, since we are not studying the chemical composition, potassium Phosphate (K2HPO4) and Sodium aluminate (NaAlO2) was been used to make the basic electrolyte. Potassium hydroxide (KOH) was used to adjust the conductivity of the electrolyte. Aqueous solution of 4g NaAlO2 and 10g K2HPO4 with 1L deionized water is used as the electrolyte for PEO on Ti-6Al-4V alloy.

**Table 3.2.1** Conductivity of Electrolyte in μΩ/cm Related to Number of KOH Tablets and Temperature in Celsius

| Temperature | 0 | 1 | 2 | 3 | 4 | 5 | 6 |
|---|---|---|---|---|---|---|---|
| 20 | 421 | 491 | 528 | 540 | 600 | 670 | 706 |
| 25 | 442 | 505 | 575 | 614 | 645 | 693 | 746 |
| 30 | 449 | 525 | 577 | 631 | 655 | 707 | 755 |
| 35 | 453 | 529 | 577 | 635 | 660 | 711 | 761 |
| 40 | 465 | 534 | 596 | 641 | 665 | 717 | 766 |
| 45 | 466 | 535 | 597 | 644 | 665 | 720 | 770 |
| 50 | 469 | 539 | 600 | 649 | 669 | 724 | 777 |
| 55 | 469 | 538 | 602 | 648 | 670 | 721 | 778 |
| 60 | 481 | 540 | 606 | 652 | 678 | 724 | 798 |
| 65 | 482 | 538 | 611 | 657 | 682 | 734 | 798 |
| 70 | 480 | 548 | 619 | 672 | 687 | 741 | 802 |
| 75 | 476 | 550 | 617 | 672 | 688 | 739 | 798 |

### 3.3 Design of Treatment Parameters

During the experiment, a Magna power electronic DC power source was used to provide voltage. Then connected Ti-6Al-4V with anode and graphite plate with cathode. Parallel placing the Ti-6Al-4V and graphite plate in a beaker with solution mentioned above and immerge them into the solution but don not let the electrode of DC power source contact with the solution. Increase the voltage with time estimate 1V/s until the discharge phenomenon obviously appear, then keep the voltage until the oxide layer formed (This progress usually sustains 5mins in total) and record the statistics of voltage and current change in every second.

According to the difference of the electrical models, the research divided the experiment in 3 catalogs, which are Non-bubble or little bubble without in fluence model, Bubbles with influenc model and Vapor envelope model which will be discussed in detail in next chapter.

# CHAPTER 4

## INVESTIGATING THE PARAMETER AFFECTING RESISTANCE

Three electrical model with different influence factors has been built in this research, which are model of passive oxidation film PEO stage, model of new oxidation film PEO stage and arcing PEO stage. During the experiment, two plates parallel deposited in a beaker with solution after connected with DC power source, which situation shown in figure 4.1.

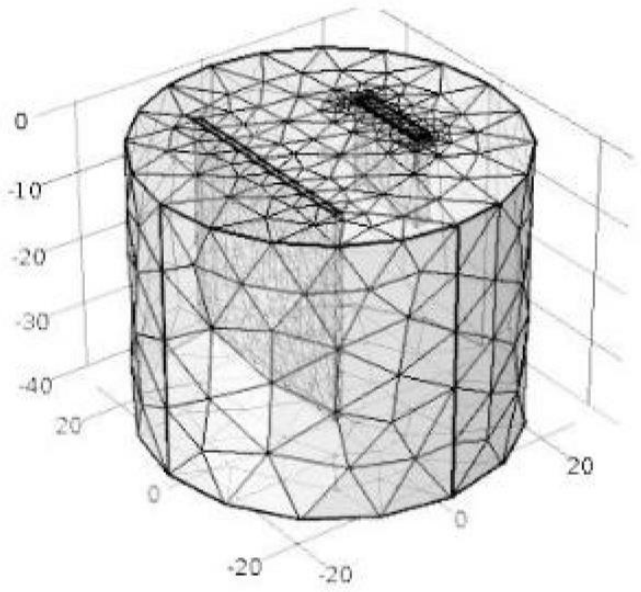


**Figure 4.1** Schematic of deposition situation

Source: Linxin Zhu. Development of plasma Eelctrolytic Deposition: Princples, Process, Properties and Simulations. (2017) 1-243.

The influence factors are what should be taken in to account to the simulation calculation. It may contain a lot, such as different parts' resistance, temperature and how to adjust the influence of bubbles emerged. Besides, costing usually formed in different situation with different experiment parameter. Sometime, the conductivity of solution is not quite well, since the current keep in a relatively low situation. If so, discharge happened with aqueous solution surrounded electrode. And we call this one nuclear boiling PEO coating. With the increase of conductivity of

solution, increasing current may cause boiling and entered into transit boiling stage. Gradually formed bubbles may cover parts of area of electrode before the coating formed. Thus, we use the second model to solve the problem and call it transit boiling PEO coating. Finally, if the current big enough to boil aqueous solution into film boiling stage, a gas envelop will emerged and we have to consider resistance of this part. Thus, we use film boiling PEO coating model to do simulation.

### 4.1 Model of Passive Oxidation Film PEO Stage

In this model, the current is small because of low conductivity of electrolyte. According to $Q=I^2Rt$, less heat was produced and is not able to boil the solution before the oxidation layer formed. Thus, only resistance of anode, cathode and electrolyte was taken into account in simulation. This model is the simplest one because what should be considered is only Ra (resistance of anode) which consist Roxidation (resistance original TiO2 on Ti-6Al-4V) and resistance of Ti-6Al-4V itself, Rc (resistance of cathord) and Re (resistance of electrolyte). Both the electrode is cuboid, so it is easy to calculate by $R=\rho L/A$ ($\rho$ is conductivity of specific material, L is length and A is area. The shape electrolyte in a beaker is a cylinder, but we consider only part between parallel electrode and we take the average area of these two electrodes as the effective area in order to use $R=\rho L/A$. What deserved to be mentioned is though there are still some bubbles produced in unclear boiling stage, they will leave the surface of electrode immediately and cause no influence. Thus, we could get the simulation result with below program (use one experiment statistic as an example.

```
>> pa=1.710e-6;pc=3.00e-3;pe=1/(422e-4); %Resistance of three parts

>> Aa=21*13.5*1e-6;Ac=35*36*1e-6;Ae=(Ac+Aa)/2; %Area of three parts

>> La=2e-3;Lc=3e-3;Le=42e-3; %Longitude of three parts
```

```
>> Ra=pa*La/Aa;

>> Rc=pc*Lc/Ac;

>> Re=pe*Le/Ae;

>> Roxidation=((1740*0.7*Aa*1e6)/38.48);

>> R=(Ra+Rc+Re+Roxidation);
```

### 4.2 Model of New Oxidation Film PEO Stage

Compared with nuclear boiling PEO Coating, more factors like temperature and bubbles should be considered because increasing current. At first, increasing temperature of electrodes were taken into account because the Joule heat produce form the increasing current. The resistance will increase since the electrodes were made of Ti-6Al-4V and graphite. The exact value of the increasing resistance could be estimated by $R=R_0(1+\alpha\Delta T)$. Where $R_0$ is resistance in 20°C, $\alpha$ is the temperature coefficient, $\Delta T$ is the change of temperature and R is the new resistance in specific temperature. Temperature mentioned above could be calculated by $Q= I^2Rt= cm\Delta T$, where c is Specific Heat Capacity, m is mass of electrodes and Q is the energy produced by increasing current. Thus, we could estimate all the resistance in different temperature (Ra, Rc, Re and Roxidation).

However, after the experiment, we found this kind of system is complex and reasonless, because heat transfer was omitted and hard to calculate. In addition, although electrodes did have temperature increase, liquid solution would cool down them and always maintain the surface temperature below 100°C, which illustrate the resistance of electrodes won't change too much with increasing current. Actually, most of the heat were transfer into electrolyte and air. Thus, resistance change of electrodes could be ignored and the most important factor influence current curve is

resistance change of electrolyte. Moreover, the passive oxidation file of Ti-6Al-4V is gradually dissolve after applied voltage increase to 110V. Basic on this, the reasonable model could be built, which is approximately approach to the experimental result.

```
>> pa=1.710e-6;pc=3.00e-3;pe=1/((1000)*1e-4);

>> Aa=20*13.5*1e-6;Ac=42*36*1e-6;Ae=(Ac+Aa)/2;

>> La=2e-3;Lc=3e-3;Le=37e-3;

>> Ra=pa*La/Aa;

>> Rc=pc*Lc/Ac;

>> Re=pe*Le/Ae;

>> Roxidation=((1740*0.7*Aa*1e6)/38.48);

>> Ro=Roxidation.*(V<110)+(Roxidation-(Roxidation/(200-110))*(V-110)).*(V>=110);

>> R=Ra+Re+Rc+Ro;

>> I=V./R;
```

### 4.3 Model of Arcing PEO Stage

After the passive oxidation film completed dissolved, new oxidation film start to form. Although the thickness of new film is nearly same as the original one, the resistivity against DC current is significantly 20 times weaker than original one [60]. In the observation of experiment, in medium voltage increase speed, new oxidation film will form between 200V-240V gradually. Compared with former 2 models, composition of resistance should take shifting of new oxidation film in to account. The consequent resistance will keep constant and significantly reduce under the influence

of temperature. What should be mentioned is temperature at this term measured by thermometer is 60 degree is Celsius. But conductivity is much higher than it should be compares to statistic in a specific measurement experiment. It illustrates that complex heat transfer happen in system. In this model, heat flux part did not concern. Simulated statistic is approximately approach to the experimental one.

```
>> pa=1.710e-6;pc=3.00e-3;pe=1/((1065)*1e-4);

>> Aa=20*13.5*1e-6;Ac=36*36*1e-6;Ae=(Ac+Aa)/2;

>> La=2e-3;Lc=3e-3;Le=37e-3;

>> Ra=pa*La/Aa;

>> Rc=pc*Lc/Ac;

>> Re=pe*Le/Ae;

>> Roxidation=((1740*0.7*Aa*1e6)/38.48);

>> Rno=0.*(V<200)+(0.05*Roxidation/(240-200))*(V-
200).*(V>=200&V<240)+(0.05*Roxidation).*(V>=240);

>> Ro=Roxidation.*(V<110)+(Roxidation-(Roxidation/(200-110))*(V-
110)).*(V>=110&V<=200)+0.*(V>200);

>> R=Ra+Re+Rc+Ro+Rno;

>> I=V./R;
```

# CHAPTER 5

## RESULT AND DISCUSSION

Few papers focus on the simulation in PEO progress, and nearly all of them pay their attention on theory only or focus on the experiment result only. In this passage, we try to consider all of the element which influence the result, building up model according to physics law. Then, we use real experimental statistic to examine whether it can be used or not. In other to demonstrate the model is not a coincident just meeting one specific situation, a lot of experiments were taken.

In terms of statistics deposit, we used a camera to record real applied voltage and current since beginning to finish. Then, stop the video in every second and record real voltage and current in pictures. With these stuffs, three charts were draw by MATLAB (Applied Voltage Change with time, Current change with time and Voltage-current curve).

Statistics of nuclear boiling PEO coating analyzing showing below

## 5.1 Passive Oxidation Film Stage Analyzing

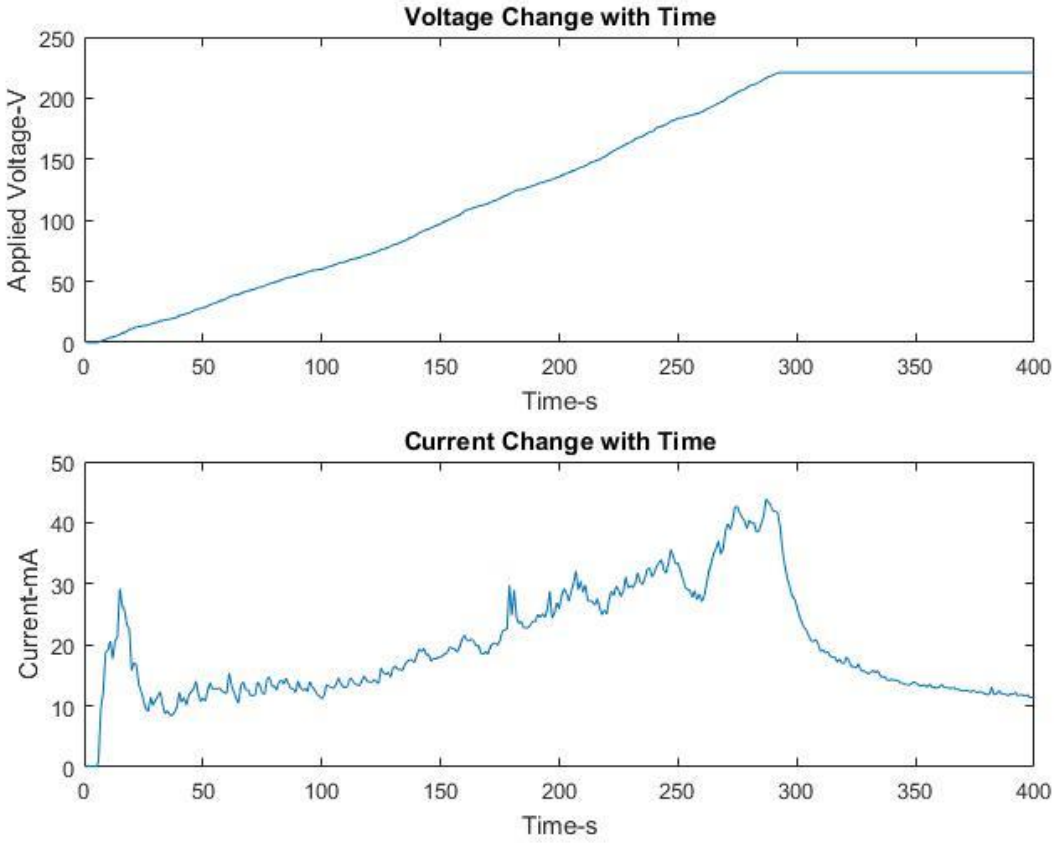


**Figure 5.1.1 (a)** Schematic of Voltage change with time and current change with time. The conductivity of experiment is 422μΩ/cm.

In figure 5.1.1 (a), we could see voltage gradually change from 0 to 221V in 293 seconds which is slow enough to relief hysteresis of current due to plasma produced form increasing voltage needs time to penetrate the oxidation layer. The corresponding current has a burst at the beginning then back to around 10mA at the moment of 25 second, then is gradually grow up to 41.5mA before voltage keep constant. On U-I curve shows in 5.1.1(b), it is obviously that the whole curve increases in the liner relation, which slope represent resistance. The slope of simulated line is approximately same.

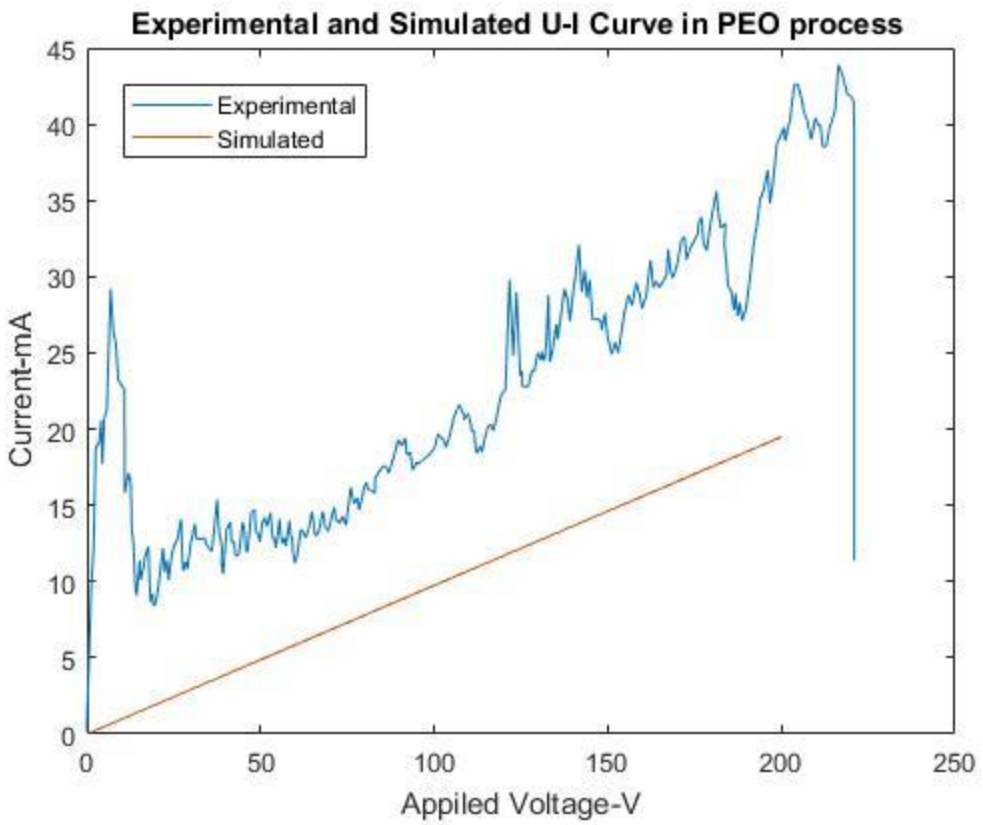


**Figure 5.1.1(b)** Schematic of U-I curve. The conductivity of experiment is 422μΩ/cm.

The burst at the beginning is because the sample was immediately used after grinding machine. The oxidation layer did not form firmly, which has less value of resistance compared with long-time formed oxidation. After the connected to DC power source, the sample was soon be oxidized. Thus, the current would sharp rise first then back to the regular value. The reason why the curve presents a serrated shape is control of increasing applied voltage is manual operated, turning a wheel by hand. That means the increasing rate could not be absolutely constant. Once the voltage keeps constant or increase in a slow rate, the current will drop immediately, which cause the curve into a serrated shape. The reason why the line start form 10mA is still under consideration.

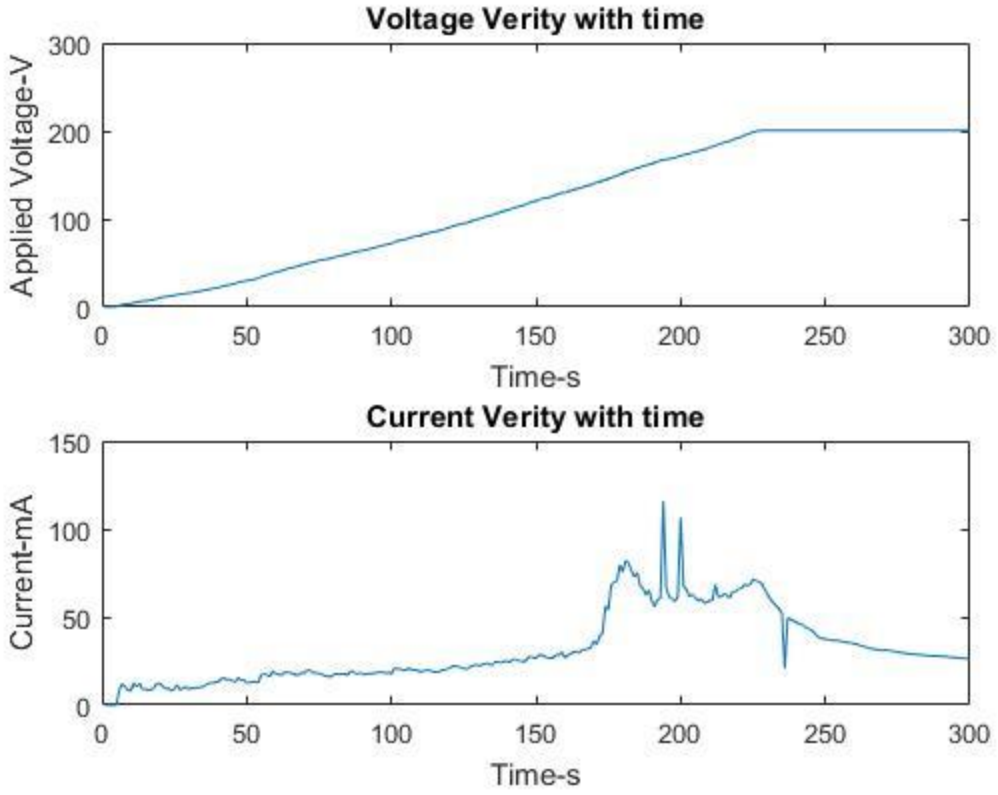


**Figure 5.1.2 (a)** Applied Voltage Change with time, Current change with time and Voltage-current curve of 451μS/cm.

In this experiment shows as figure 5.1.2 (a) and 5.1.2 (b). Applied voltage gradually moved from 0 to 200.7V in 227 seconds with a slow increase rate. Then, it kept constant at 200.7V after 227 second until finish. The current increase steady until around 175mA, connecting a sharp increase and 2 bursts before it went down. The U-I curve at this conductivity is nearly the same trend with current curve, which has sharp increase and two bursts at the end. The slope of U-I curve presents the resistance which is nearly same as the simulated one.

There is no burst at the beginning is because Ti-6Al-4V sample had been grinded for a relative long time, causing firmly oxidation coating existed before experiment. The sharp increase is due to big arc discharge occurred and the two bursts may cause by digital change when purse the video. The non-straight creep line is because hand-controlled wheel.

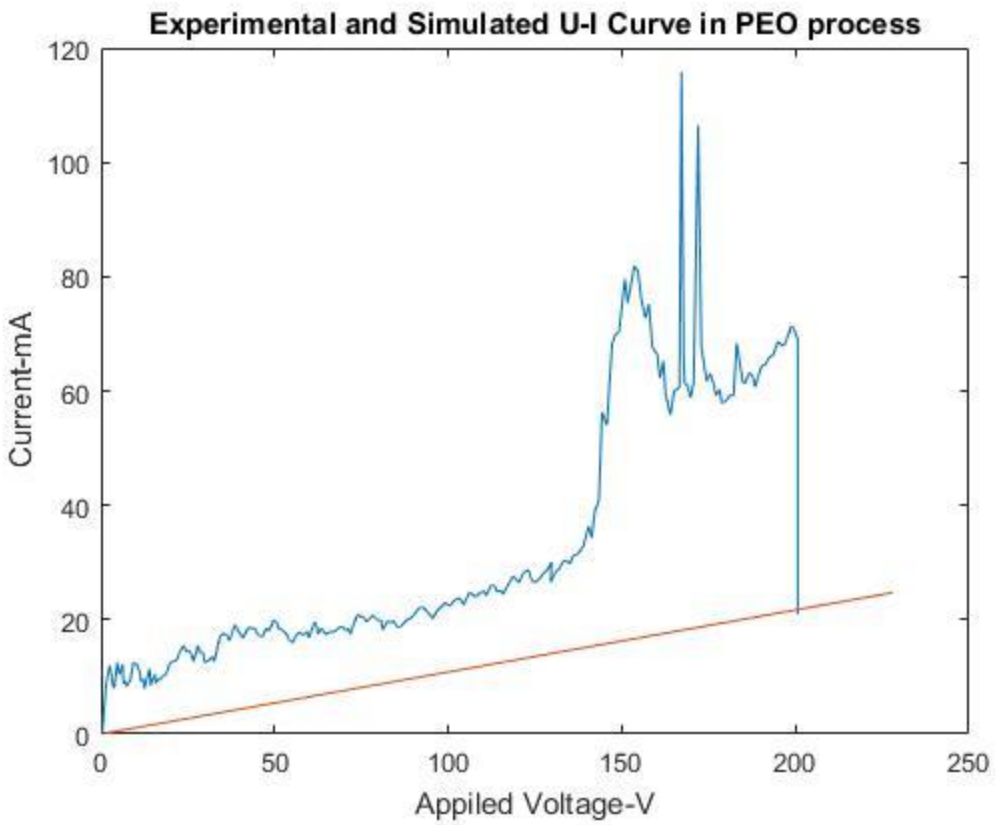


**Figure 5.1.2 (b)** Schematic of U-I curve. The conductivity of experiment is 451μΩ/cm.

In figure 5.1.3 (a), we could see voltage gradually change from 0 to 200.5V in 193 seconds which is middle increase speed. The corresponding current has a burst at the beginning then back to around 10mA at the moment of 25 second, then is gradually grow up to 36.4mA before voltage keep constant. On U-I curve shows in 5.1.3(b), the whole curve increases in the liner relation except a hill in the middle, which slope represent resistance. The slope of simulated line is approximately same.

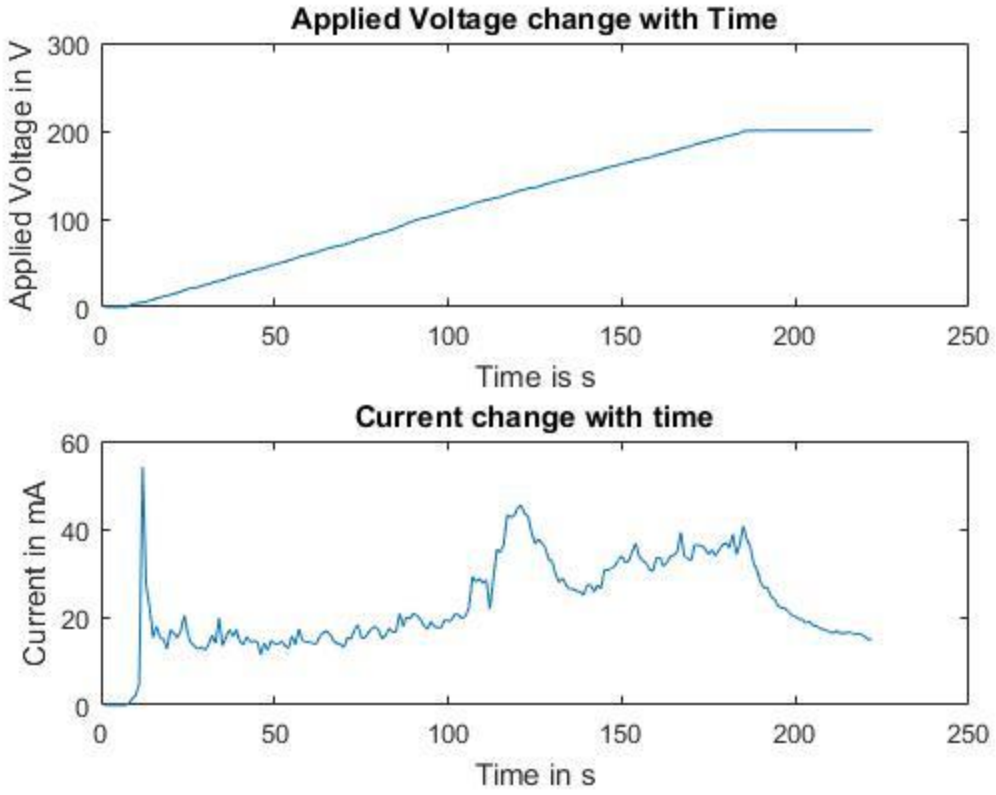


**Figure 5.1.3 (a)** Applied Voltage Change with time, Current change with time and Voltage-current curve of 439µS/cm.

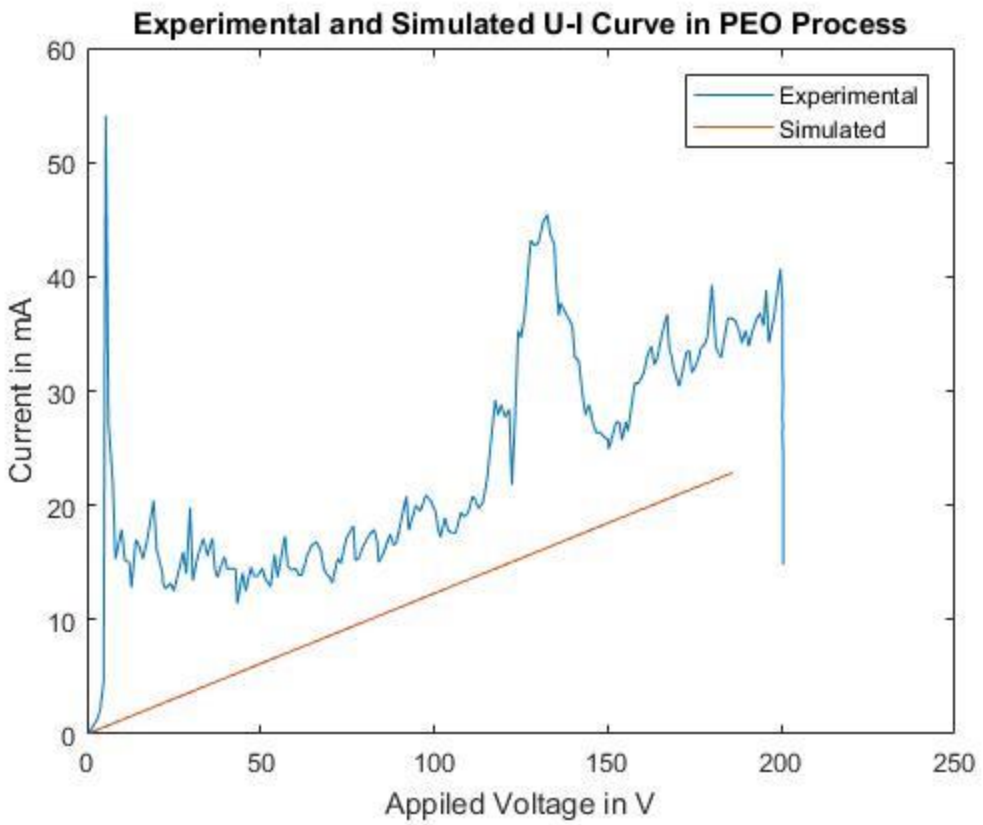


**Figure 5.1.3 (b)** Schematic of U-I curve. The conductivity of experiment is 439μΩ/cm.

The burst at the beginning is because the sample was immediately used after grinding machine. The reason why the curve presents a serrated shape is control of increasing applied voltage is manual operated, turning a wheel by hand. That means the increasing rate could not be constant. Once the voltage keeps constant or increase in a slow rate, the current will drop immediately, which cause the curve into a serrated shape. The reason why the line start form 10mA is still under consideration. The hill in the middle may cause by overspeed increase of voltage or big arc discharge due to surface roughness.

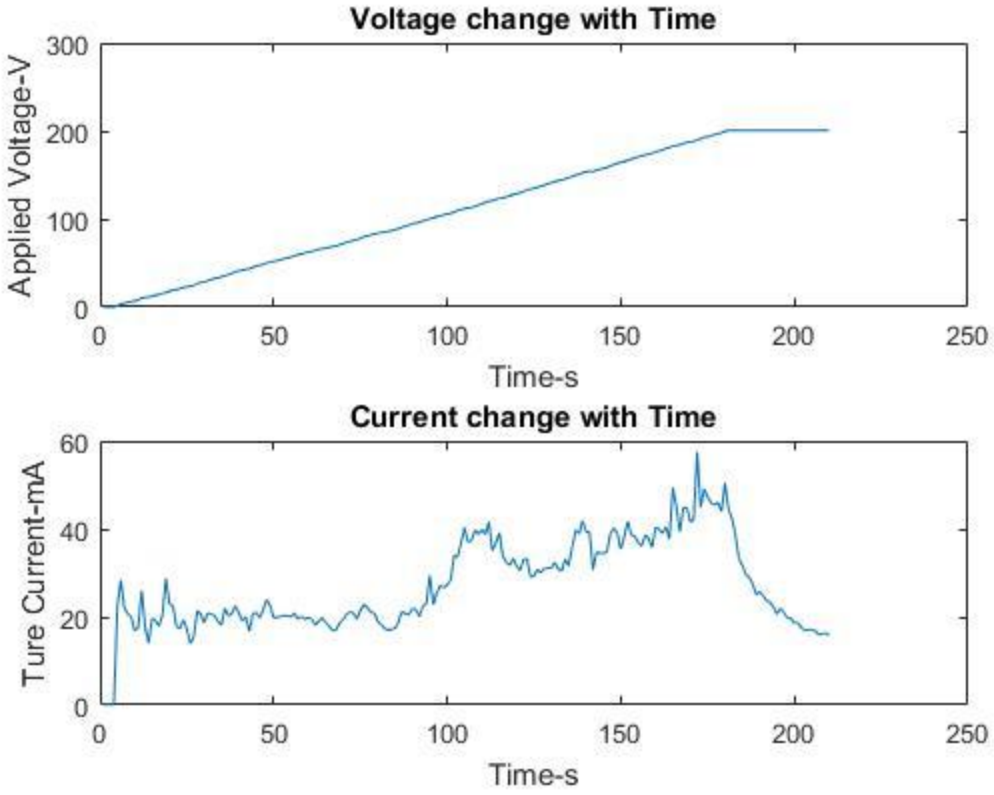


**Figure 5.1.4 (a)** Applied Voltage Change with time, Current change with time and Voltage-current curve of 409μS/cm.

In this experiment shows as figure 5.1.4 (a) and 5.1.4 (b). Applied voltage gradually moved from 0 to 200.7V in 181 seconds with a middle increase rate. Then, it kept constant at 200.7V after 227 second until finish. The current increase steady until around 44.5 mA and went down after the voltage keep constant. In the middle, there is small hill. The U-I curve at this conductivity is nearly the same trend with current curve, which has a hill at the middle and fall at the end. The slope of U-I curve presents the resistance which is nearly same as the simulated one.

There is no burst at the beginning is because Ti-6Al-4V sample had been grinded for a relative long time, causing firmly oxidation coating existed before experiment. The hill in the middle may cause by overspeed increase of voltage or big arc discharge due to surface roughness. The sharp increase is due to big arc discharge occurred. The non-straight creep line is because

hand-controlled wheel. Fall at last was influenced by increasing thick of oxidation coating once the voltage keep constant.

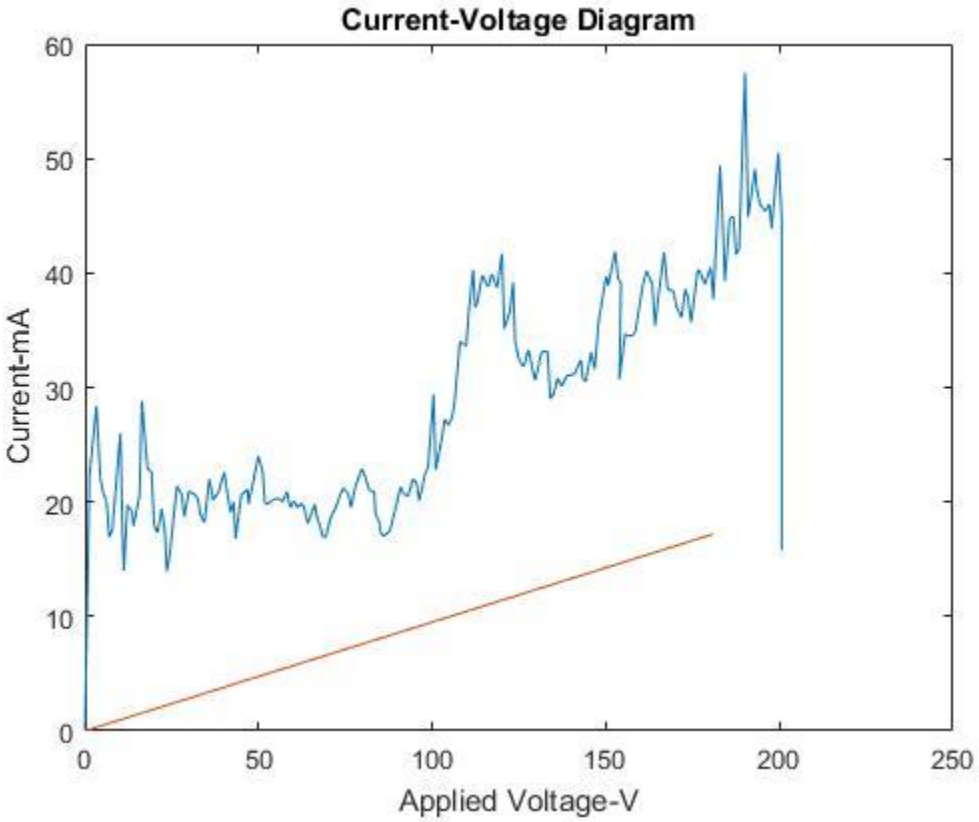


**Figure 5.1.4 (b)** Schematic of U-I curve. The conductivity of experiment is 409μΩ/cm.

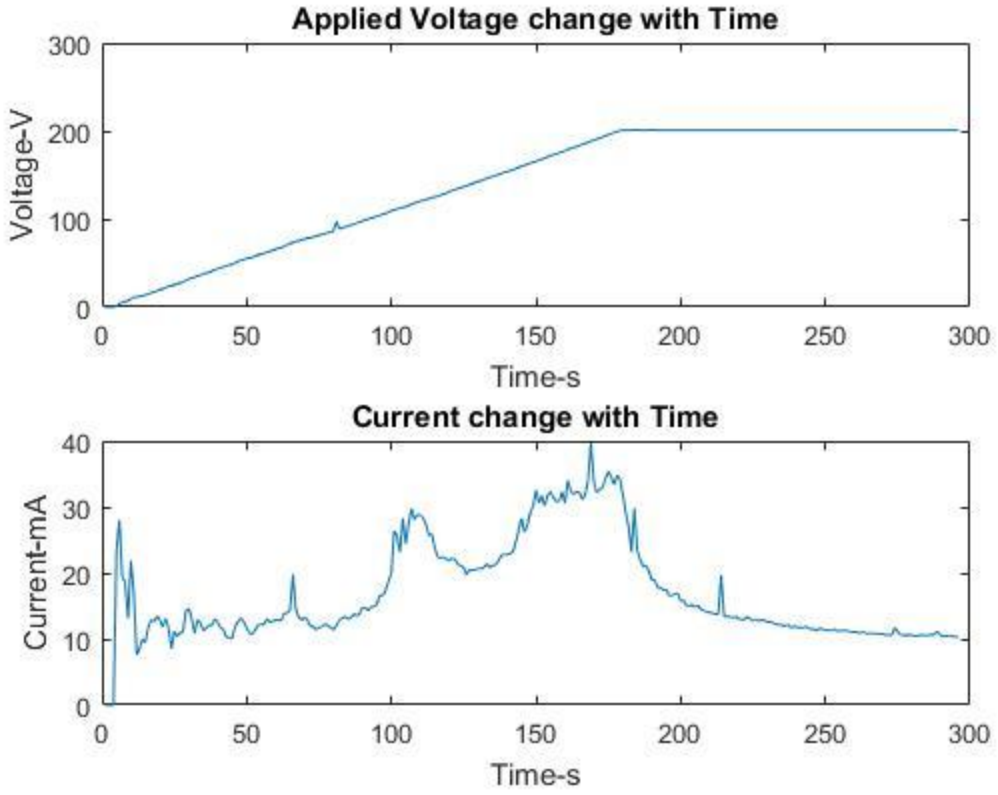


**Figure 5.1.5 (a)** Applied Voltage Change with time, Current change with time and Voltage-current curve of 457μS/cm.

In figure 5.1.5 (a), we could see voltage gradually change from 0 to 200.8V in 180 seconds which is middle increase speed. The corresponding current has a burst at the beginning then back to around 10mA at the moment of 10 second, then is gradually grow up to 32mA before voltage keep constant. On U-I curve shows in 5.1.5 (b), the whole curve increases in the liner relation except a hill in the middle, which slope represent resistance. The slope of simulated line is approximately same.

The burst at the beginning is because the sample was immediately used after grinding machine. The reason why the curve presents a serrated shape is control of increasing applied voltage is manual operated, turning a wheel by hand. That means the increasing rate could not be constant. Once the voltage keeps constant or increase in a slow rate, the current will drop

immediately, which cause the curve into a serrated shape. The reason why the line start form 10mA is still under consideration. The hill in the middle may cause by overspeed increase of voltage or big arc discharge due to surface roughness.

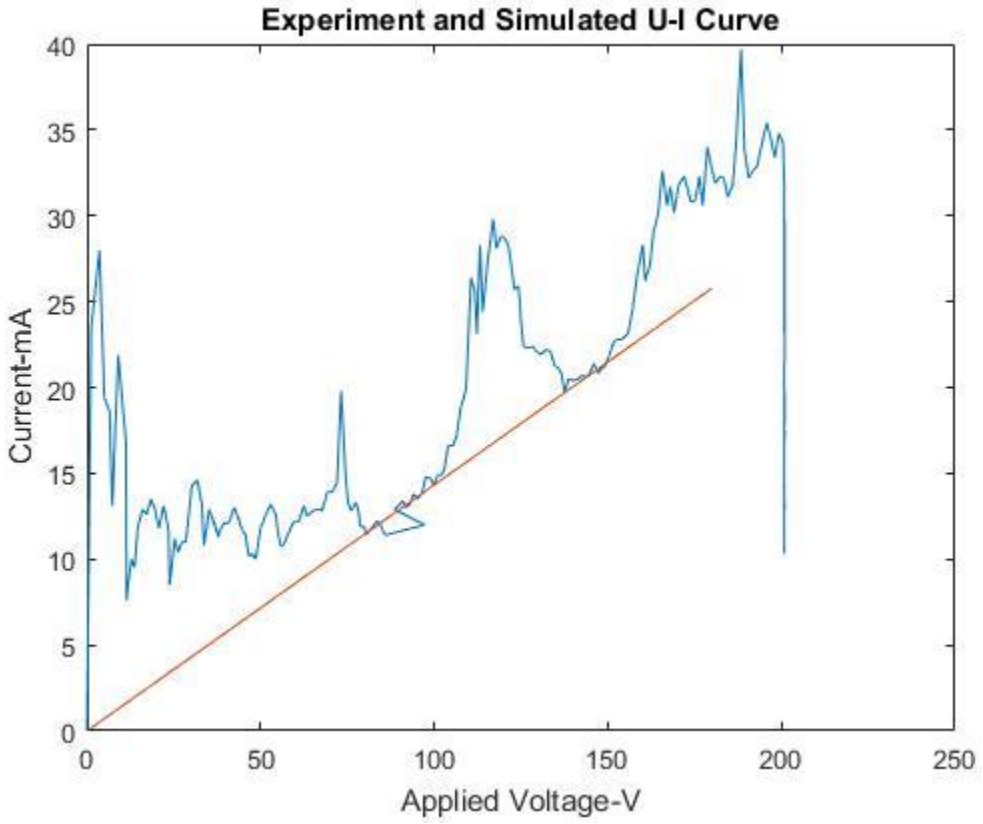


**Figure 5.1.5 (b)** Schematic of U-I curve. The conductivity of experiment is 457μΩ/cm.

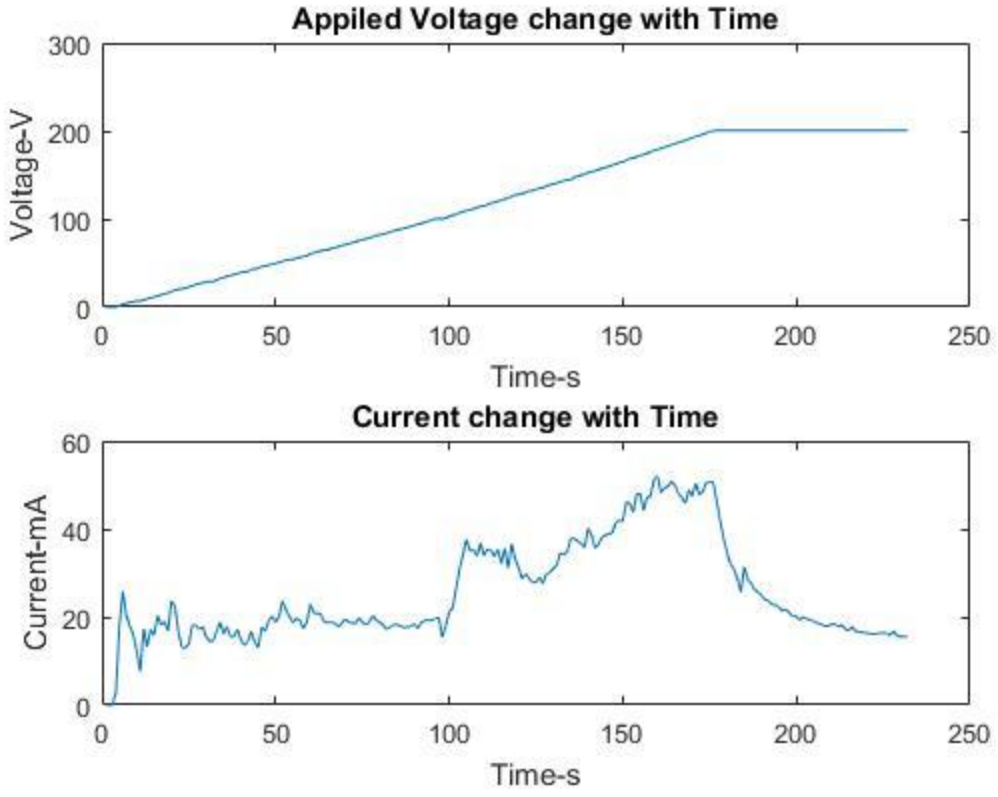


**Figure 5.1.6 (a)** Applied Voltage Change with time, Current change with time and Voltage-current curve of 461μS/cm.

In figure 5.1.6 (a), we could see voltage gradually change from 0 to 200.5V in 177 seconds which is middle increase speed. The corresponding current has a burst at the beginning then back to around 12mA at the moment of 8 second, then is gradually grow up to 50.6mA before voltage keep constant. On U-I curve shows in 5.1.6 (b), the whole curve increases in the liner relation except a hill in the middle, which slope represent resistance. The slope of simulated line is approximately same.

The burst at the beginning is because the sample was immediately used after grinding machine. The reason why the curve presents a serrated shape is control of increasing applied

voltage is manual operated, turning a wheel by hand. That means the increasing rate could not be constant. Once the voltage keeps constant or increase in a slow rate, the current will drop immediately, which cause the curve into a serrated shape. The reason why the line start form 10mA is still under consideration. The hill in the middle may cause by overspeed increase of voltage or big arc discharge due to surface roughness.

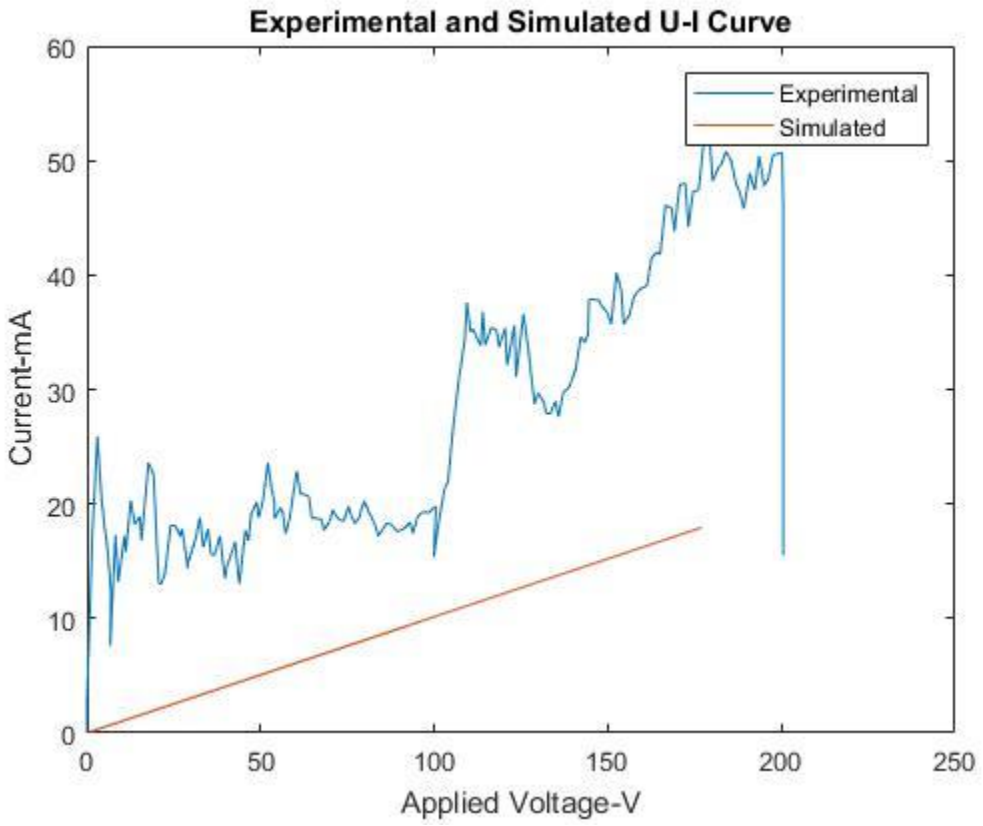


**Figure 5.1.6 (b)** Schematic of U-I curve. The conductivity of experiment is 461μΩ/cm.

## 5.2 Transition Boiling PEO Coating Analyzing

We could see, in figure 5.2.1 (a), the voltage increases from 0 to 251V in 212 seconds in a liner trend, which is a relatively slow speed. Then, the voltage keep constant in 251V after that. The current increase in a liner trend slowly from 0 to approximately 110s followed by a small hill. After that, there is a sharp increase until applied Voltage keep constant. In U-I curve showed in figure 5.2.1 (b), the whole trend is like current curve, which increase gradually like flat line before 110V. Then a small hill followed by a sharp increase appeared until 230V with a fluctuating platform at the end.

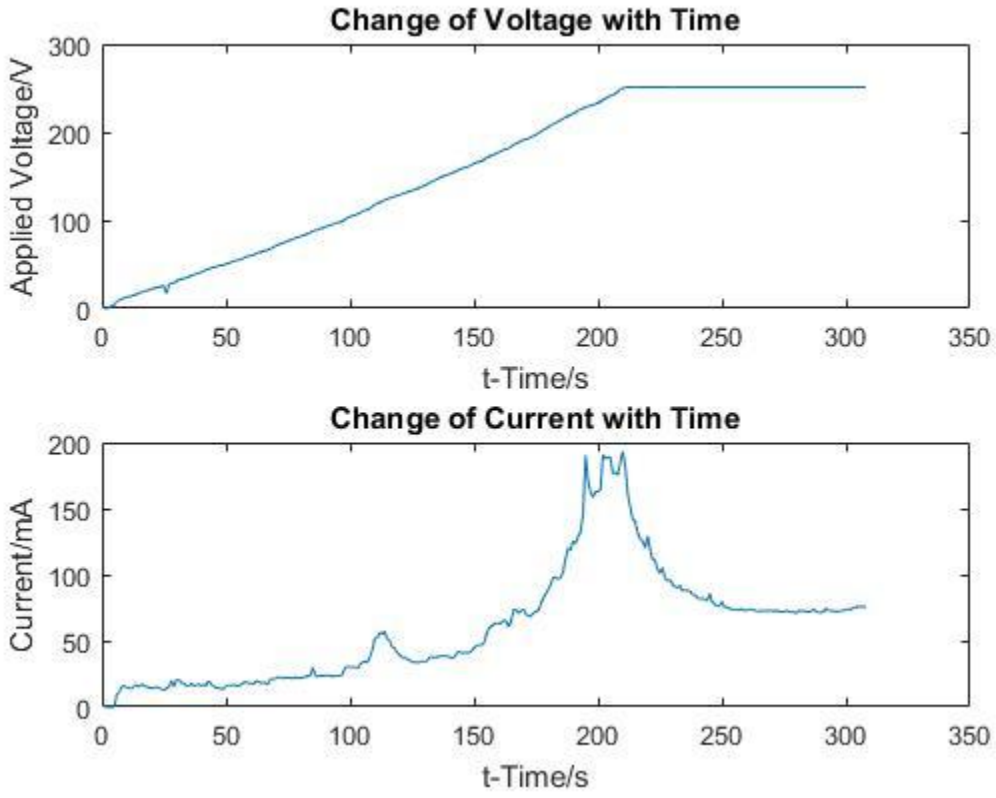


**Figure 5.2.1 (a)** Applied Voltage Change with time, Current change with time and Voltage-current curve of 580μS/cm.

The flat slope mainly causes by constantly or slightly change total resistance of electrodes, electrolyte and passive oxidation film. Then, sparking discharge make hill appeared and passive oxidation film start dissolved and will vanished in around 200V if increasing rate in a moderate speed. Thus, the total resistance will decrease and current will sharp increase. The slope of U-I curve represents reciprocal of resistance. The constant voltage after 200V make new thinner passive oxidation film forms again.

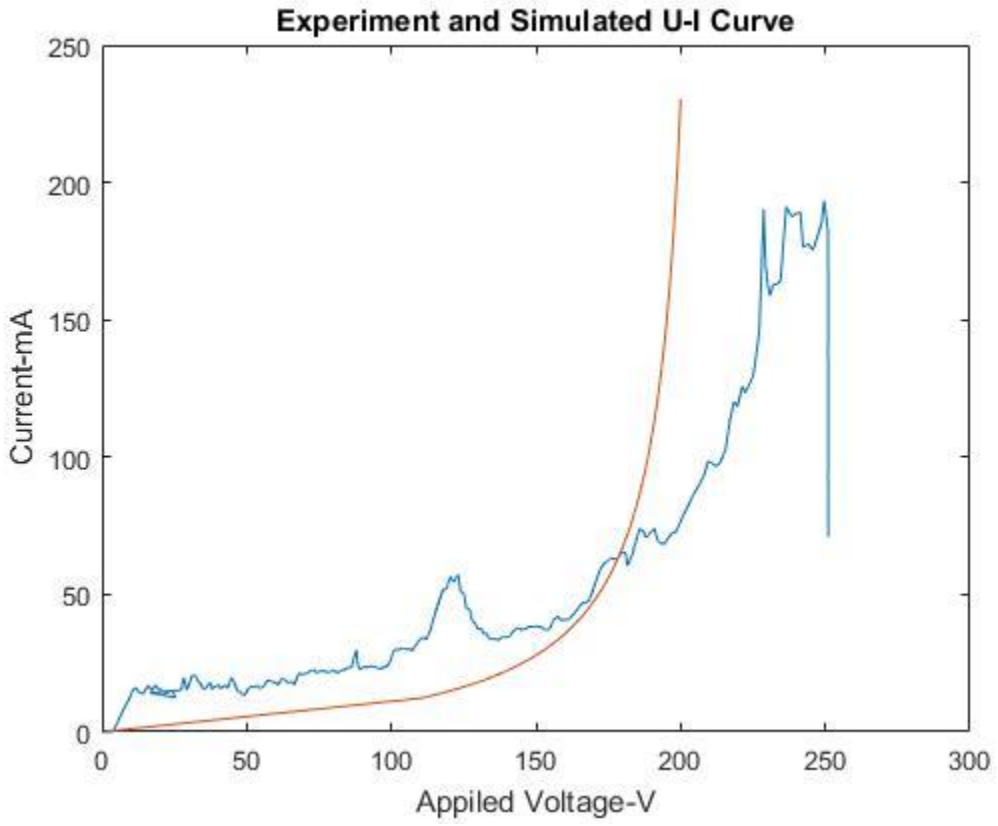


**Figure 5.2.1 (b)** Schematic of U-I curve. The conductivity of experiment is 580μΩ/cm.

We could see, in figure 5.2.2 (a), the voltage increases from 0 to 296V in 220 seconds in a liner trend, which is a relatively quick speed. Then, the voltage drops to 0 after that because of overheat. The current increase in a liner trend slowly from 0 to approximately 110s followed by a small hill. After that, there is a sharp increase until 170s, followed by decrease before another rise. In U-I

curve showed in figure 5.2.2 (b), the whole trend is like current curve, which increase gradually like flat line before 110V. Then a sharp increase appeared until 200V with a decrease before a continuously increase at the end.

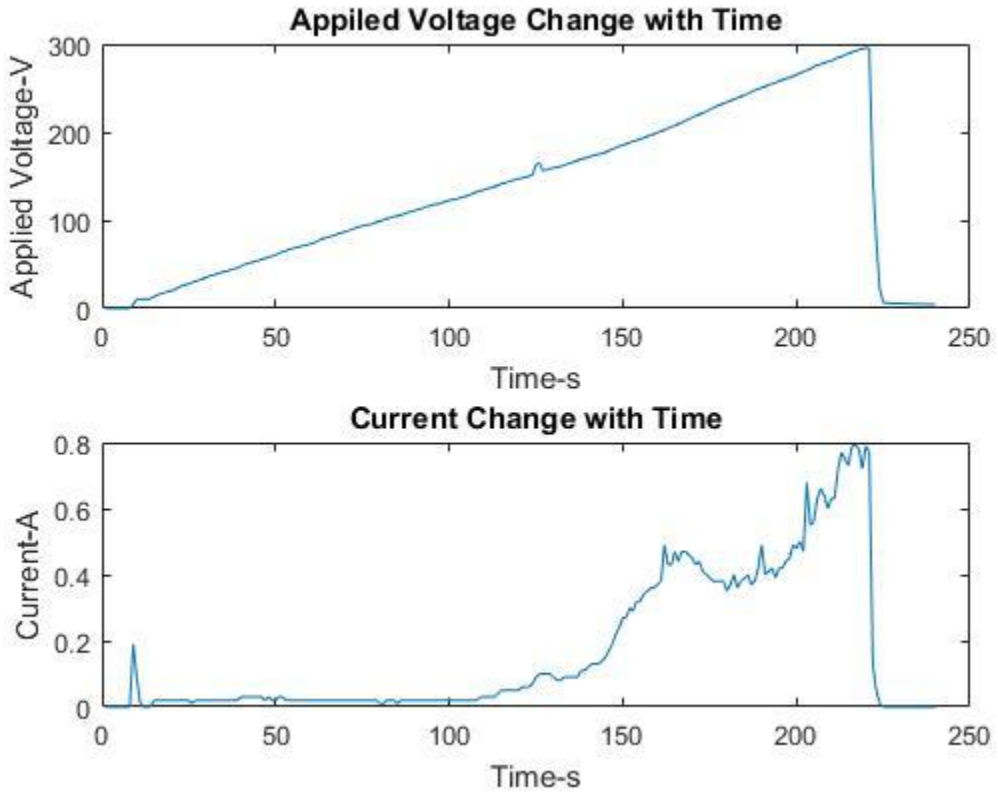


**Figure 5.2.2 (a)** Applied Voltage Change with time, Current change with time and Voltage-current curve of 900μS/cm.

The flat slope mainly causes by constantly or slightly change total resistance of electrodes, electrolyte and passive oxidation film. Then, sparking discharge make hill appeared and passive oxidation film start dissolved and will vanished in around 200V if increasing rate in a moderate speed. Thus, the total resistance will decrease and current will sharp increase. The slope of U-I curve represents reciprocal of resistance. The resistance increase again is because the new oxidation layer is form again. Simulated curve is approximately meet the experimental curve.

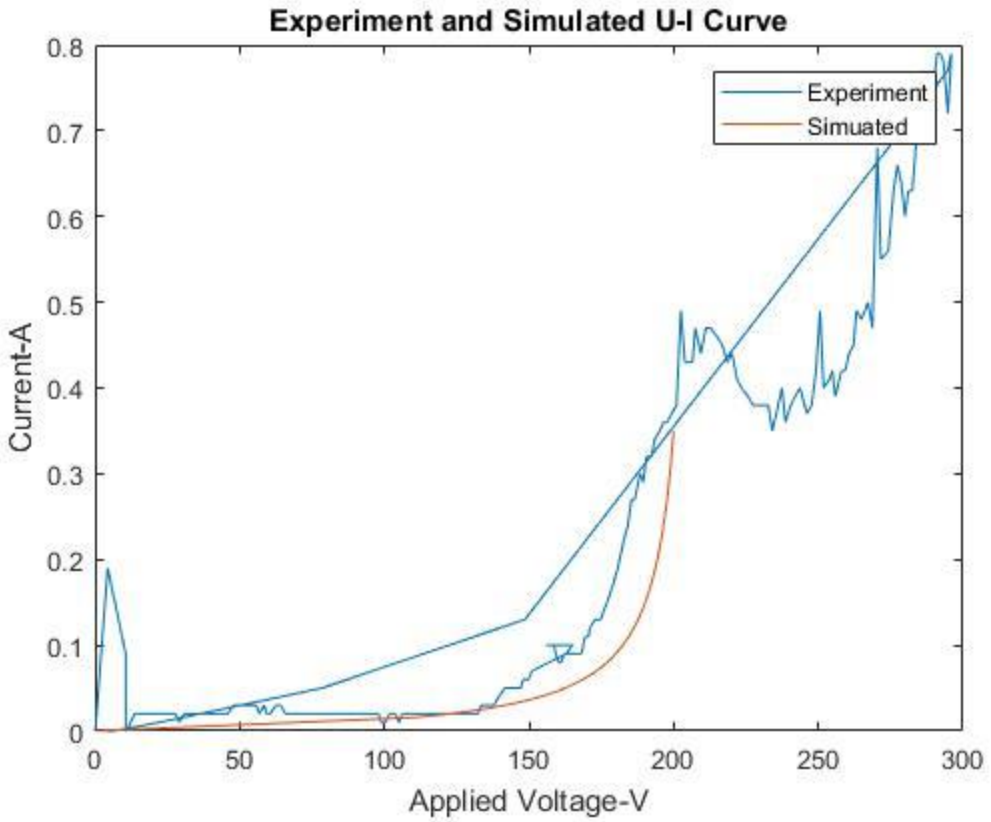


**Figure 5.2.2 (b)** Schematic of U-I curve. The conductivity of experiment is 900μΩ/cm.

Figure 5.2.3 (a) shows the voltage increases from 0 to 231.2V in 166 seconds in a liner trend, which is a quick speed. Then, the voltage keep constant in 231.3V after that. The current increase in a liner trend slowly from 0 to approximately 110s followed by a small burst. After that, there is a sharp increase until applied Voltage keep constant. A quick drop followed by al liner increase with serrated shape at the end. In U-I curve showed in figure 5.2.3 (b), the whole trend is like current curve, which increase gradually like flat line before 110V. Then a small hill followed by a sharp increase appeared until 240V with a fluctuating platform at the end.

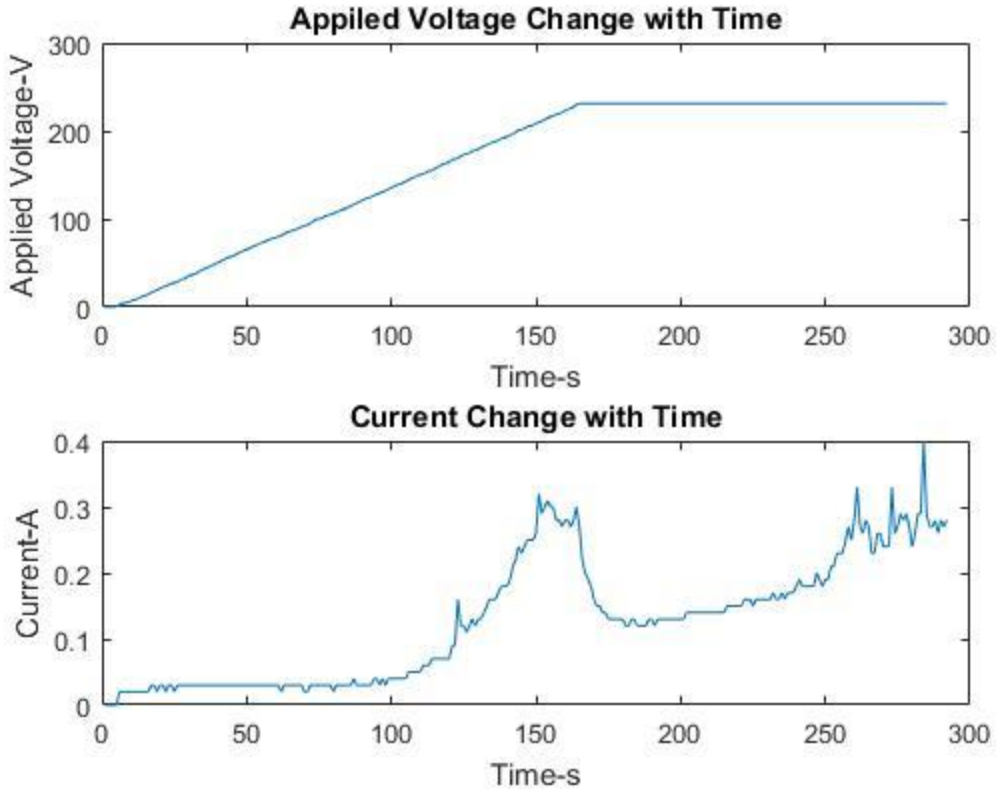


**Figure 5.2.3 (a)** Applied Voltage Change with time, Current change with time and Voltage-current curve of 700μS/cm.

The flat slope mainly causes by constantly or slightly change total resistance of electrodes, electrolyte and passive oxidation film. Then, sparking discharge make hill appeared and passive oxidation film start dissolved and will vanished in around 200V if increasing rate in a moderate speed. Thus, the total resistance will decrease and current will sharp increase. The slope of U-I curve represents reciprocal of resistance. Current keep increases after applied voltage remain constant because conductivity of electrolyte would increase with rise of temperature. The constant voltage after 200V make new thinner passive oxidation film forms again.

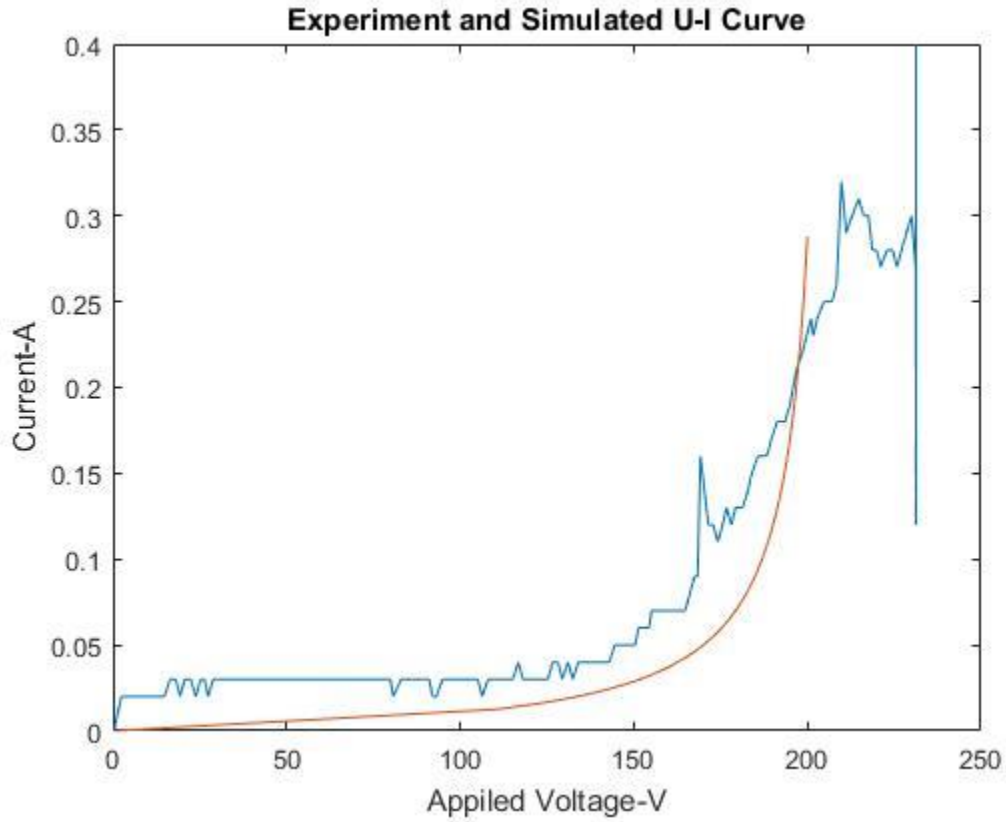


**Figure 5.2.3 (b)** Schematic of U-I curve. The conductivity of experiment is 780μΩ/cm.

We could see, in figure 5.2.4 (a), the voltage increases from 0 to 296.7V in 205 seconds in a liner trend, which is a quick speed. Then, the voltage drops to 0 after that because of DC power source overheat. The current increase in a liner trend slowly from 0 to approximately 110s followed by a small hill. After that, there is a sharp increase until 170s, followed by decrease before another rise. In U-I curve showed in figure 5.2.4 (b), the whole trend is like current curve, which increase gradually like flat line before 110V. Then a sharp increase appeared until 200V with a decrease before a continuously increase at the end.

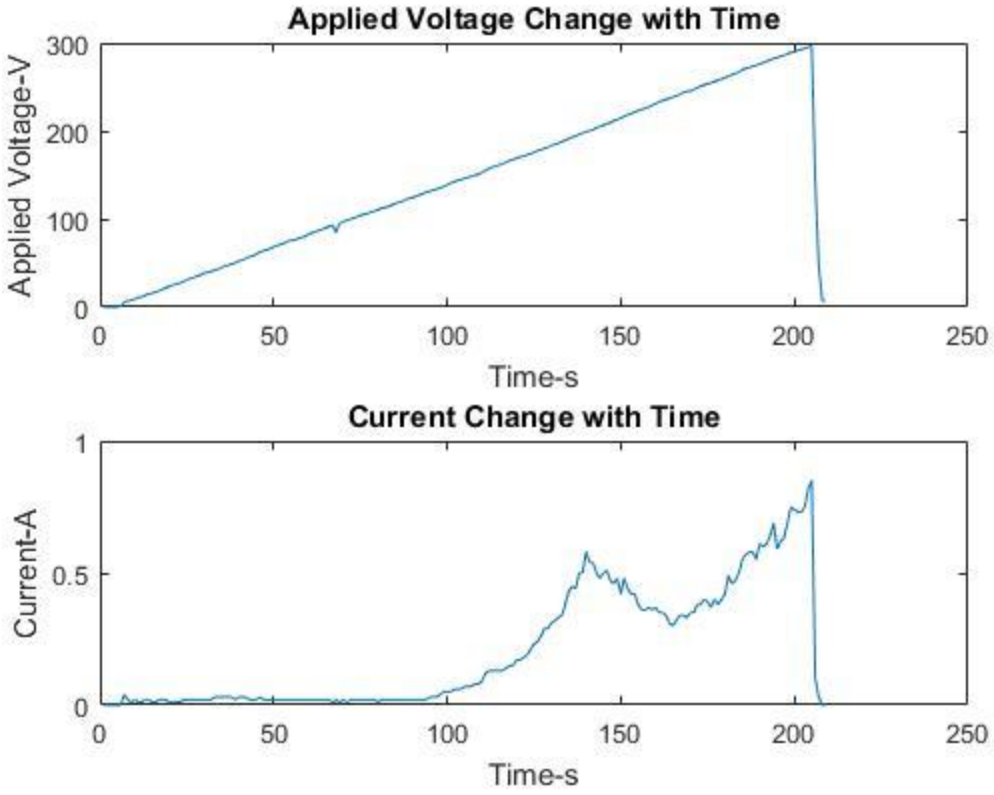


**Figure 5.2.4 (a)** Applied Voltage Change with time, Current change with time and Voltage-current curve of 780μS/cm.

The flat slope mainly causes by constantly or slightly change total resistance of electrodes, electrolyte and passive oxidation film. Then, sparking discharge make hill appeared and passive oxidation film start dissolved and will vanished in around 200V if increasing rate in a moderate speed. Thus, the total resistance will decrease and current will sharp increase. The slope of U-I curve represents reciprocal of resistance. Current keep increases after applied voltage remain constant because conductivity of electrolyte would increase with rise of temperature. The constant voltage after 200V make new thinner passive oxidation film forms again.

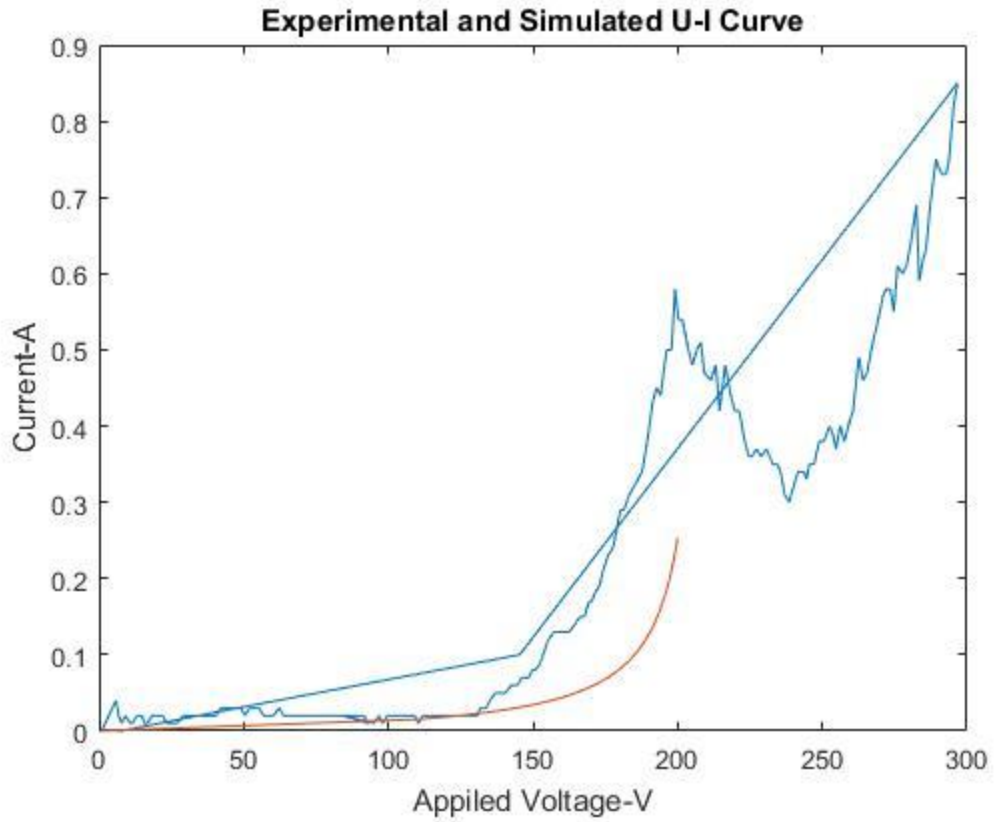


**Figure 5.2.4 (b)** Schematic of U-I curve. The conductivity of experiment is 780μΩ/cm.

Figure 5.2.5 (a) shows the voltage increases from 0 to 270V in 179 seconds in a liner trend, which is a quick speed. Then, the voltage keep constant in 270.6V after that. The current increase in a liner trend slowly from 0 to approximately 98s followed by a hill. After that, there are 2 sharp increases before applied Voltage keep constant. A relatively steady increase will be finding at the end. In U-I curve showed in figure 5.2.5 (b), the whole trend is like current curve, which increase gradually like flat line before 125V. A obviously increase would be notice at around 200V. After that, a decrease to 0.4A at 220V followed by a continuously increase until the end.

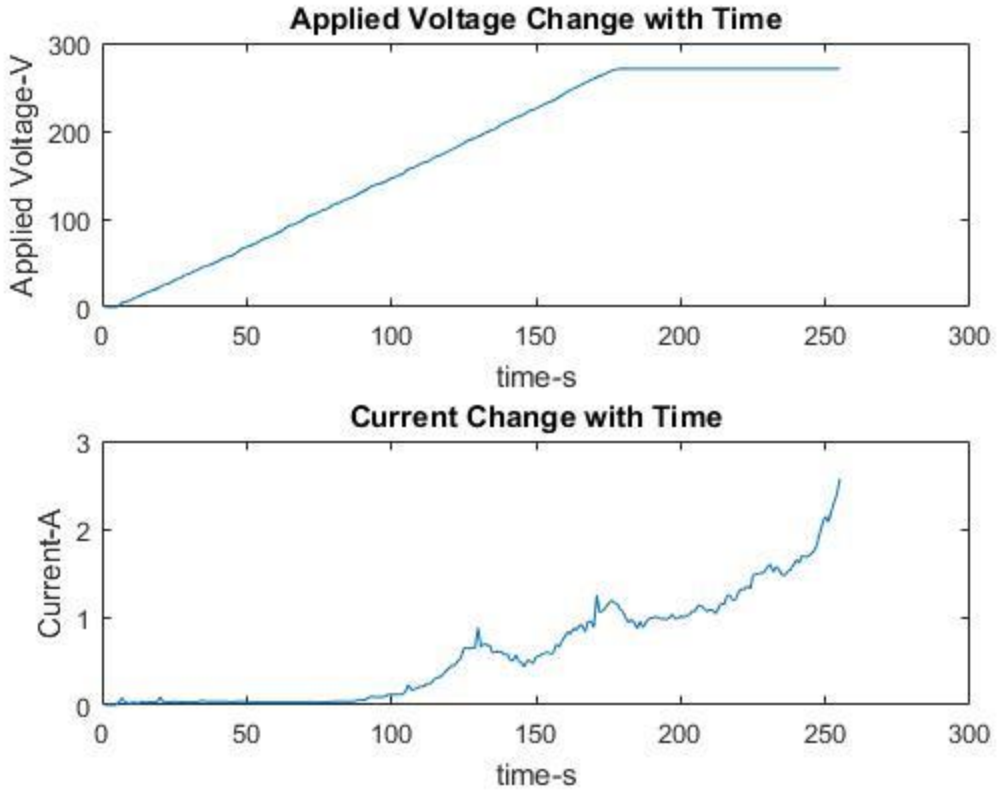


**Figure 5.2.5 (a)** Applied Voltage Change with time, Current change with time and Voltage-current curve of 1000μS/cm.

The flat slope mainly causes by constantly or slightly change total resistance of electrodes, electrolyte and passive oxidation film. Then, sparking discharge make hill appeared and passive oxidation film start dissolved and will vanished in around 200V if increasing rate in a moderate speed. Thus, the total resistance will decrease and current will sharp increase. The slope of U-I curve represents reciprocal of resistance. Current keep increases after applied voltage remain constant because conductivity of electrolyte would increase with rise of temperature. The constant voltage after 200V make new thinner passive oxidation film forms again.

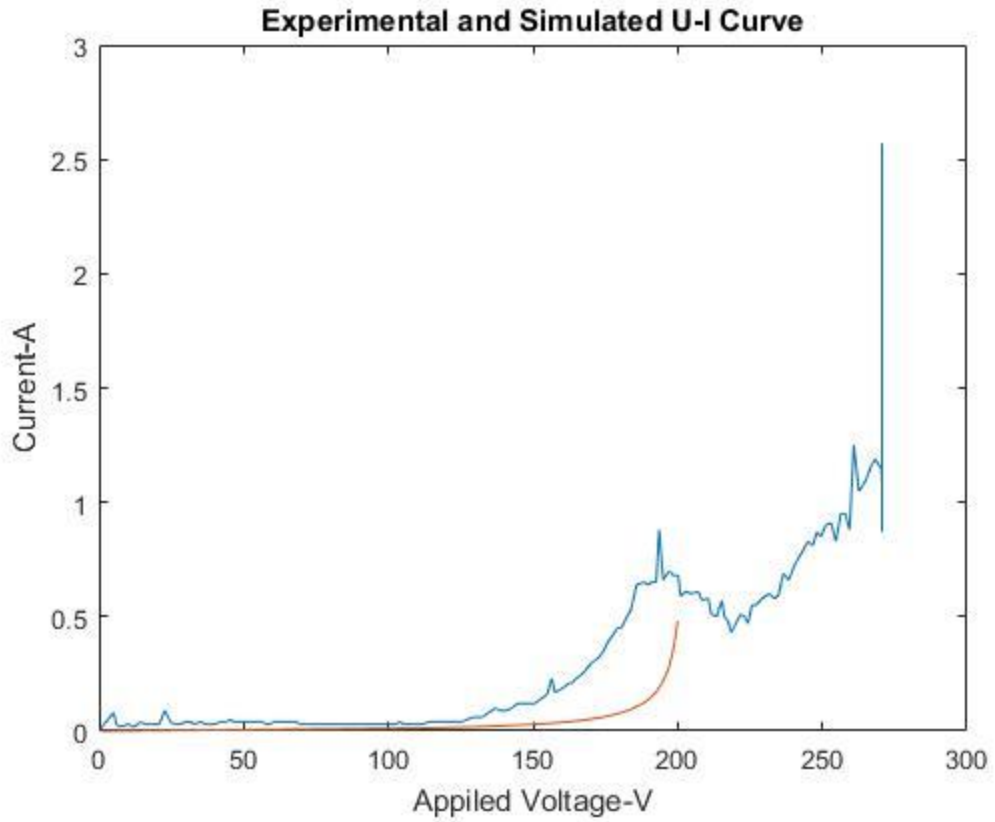


**Figure 5.2.5 (b)** Schematic of U-I curve. The conductivity of experiment is 1000μΩ/cm.

### 5.3 Film Boiling PEO Coating Analyzing

Figure 5.3.1 (a) shows the voltage increases from 0 to 296.5V in 224 seconds in a liner trend, which is a quick speed. Then, the voltage stopped because of DC source overheat. The current increase in a liner trend slowly from 0 to approximately 1.8A followed by a hill. After that, there is a sharp increase until the end. In U-I curve showed in figure 5.3.1 (b), the whole trend is like current curve, which increase gradually like flat line before 125V. A obviously increase would be notice at around 200V. After that, a decrease to 0.4A at 220V followed by a continuously sharp increase until the end.

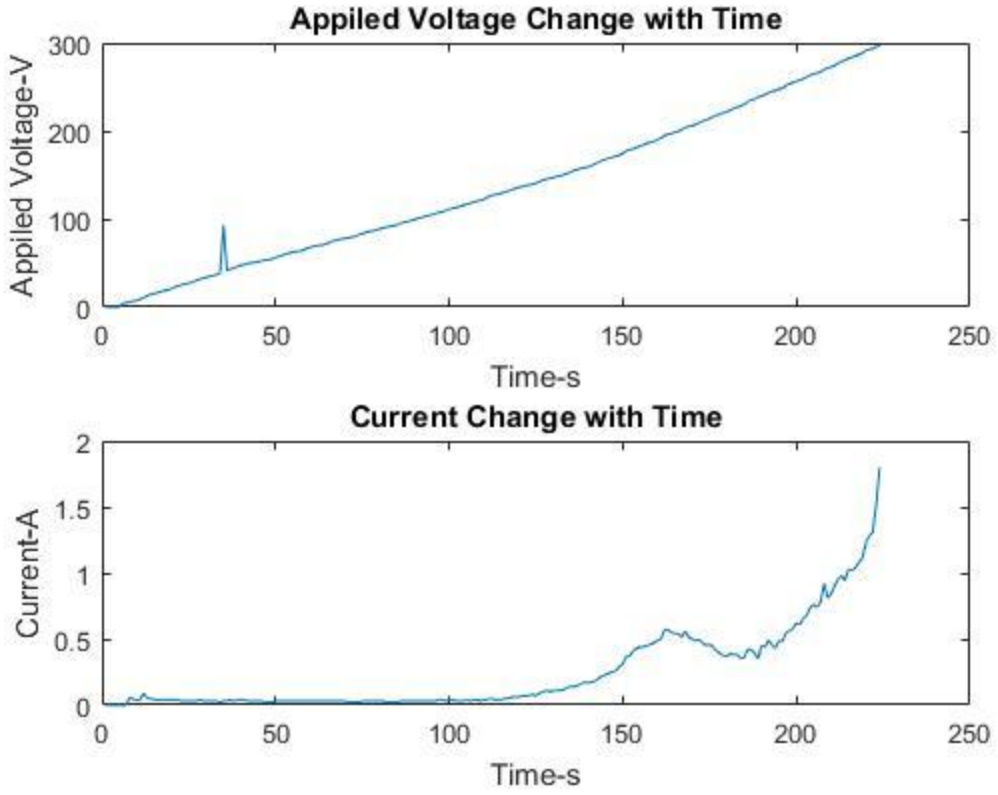


**Figure 5.3.1 (a)** Applied Voltage Change with time, Current change with time and Voltage-current curve of 1012μS/cm.

The flat slope mainly causes by constantly or slightly change total resistance of electrodes, electrolyte and passive oxidation film. Then, sparking discharge make hill appeared and passive oxidation film start dissolved and will vanished in around 200V if increasing rate in a moderate speed. Thus, the total resistance will decrease and current will sharp increase. The slope of U-I curve represents reciprocal of resistance. After that, resistance increase because of new oxidation layer formed. Then the sharp increase follows a stable slope influence by high temperature.

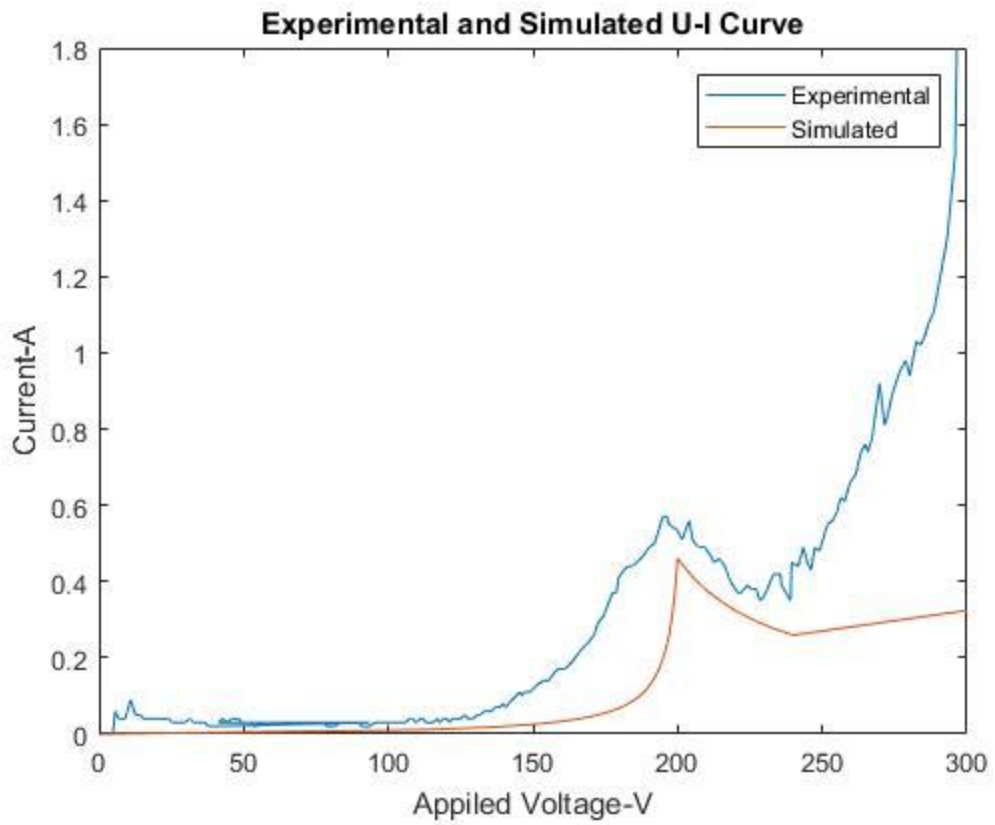


**Figure 5.3.1 (b)** Schematic of U-I curve. The conductivity of experiment is 1012μΩ/cm.

Figure 5.3.2 (a) shows the voltage increases from 0 to 260.6V in 238 seconds in a liner trend, which is a quick speed. Then, the voltage keep constant at 260.6 after that. The current increase in a liner trend slowly from 0 to approximately 0.1A at first. Then, there is a hill before fluctuate curve at the end. In U-I curve showed in figure 5.3.2 (b), the whole trend is like current curve, which increase gradually like flat line before 125V. A obviously increase would be notice at around 200V. After that, a decrease to 0.3A at 240V followed by a continuously sharp increase until the end.

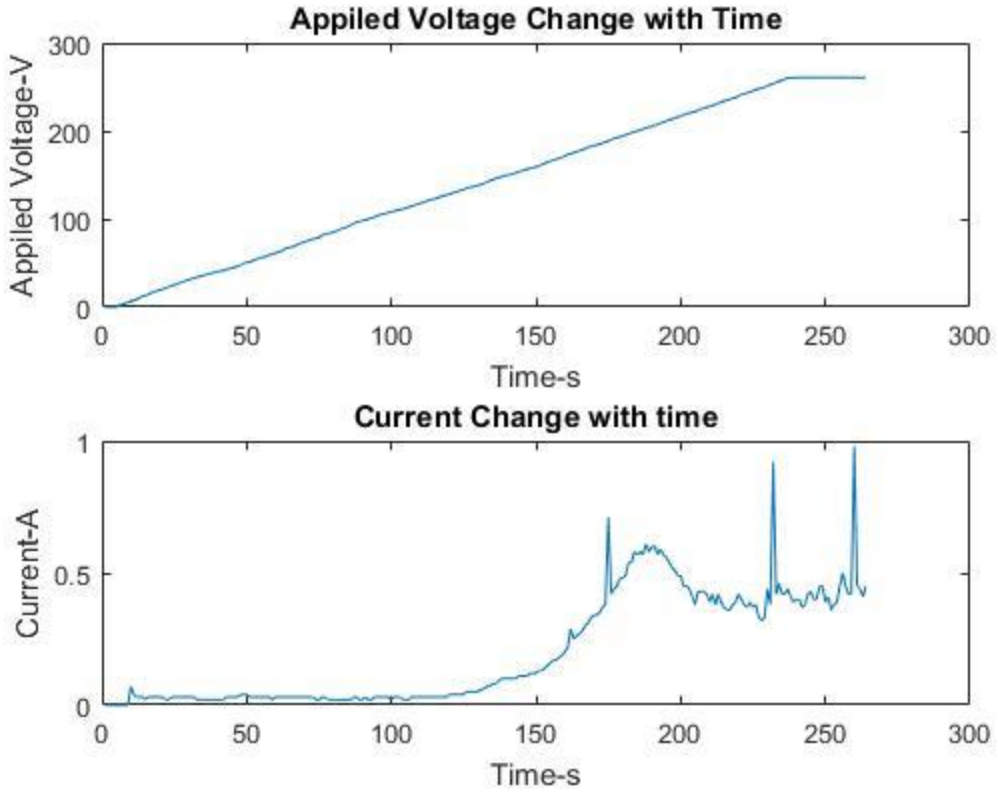


**Figure 5.3.2 (a)** Applied Voltage Change with time, Current change with time and Voltage-current curve of 890µS/cm.

The flat slope mainly causes by constantly or slightly change total resistance of electrodes, electrolyte and passive oxidation film. Then, passive oxidation film starts dissolved at 110V and will vanished in around 200V if increasing rate in a moderate speed. After that, Resistance decrease consequently because new oxidation film formed until 240V. The slope of U-I curve represents reciprocal of resistance. Then the sharp increase follows a stable slope influence by high temperature.

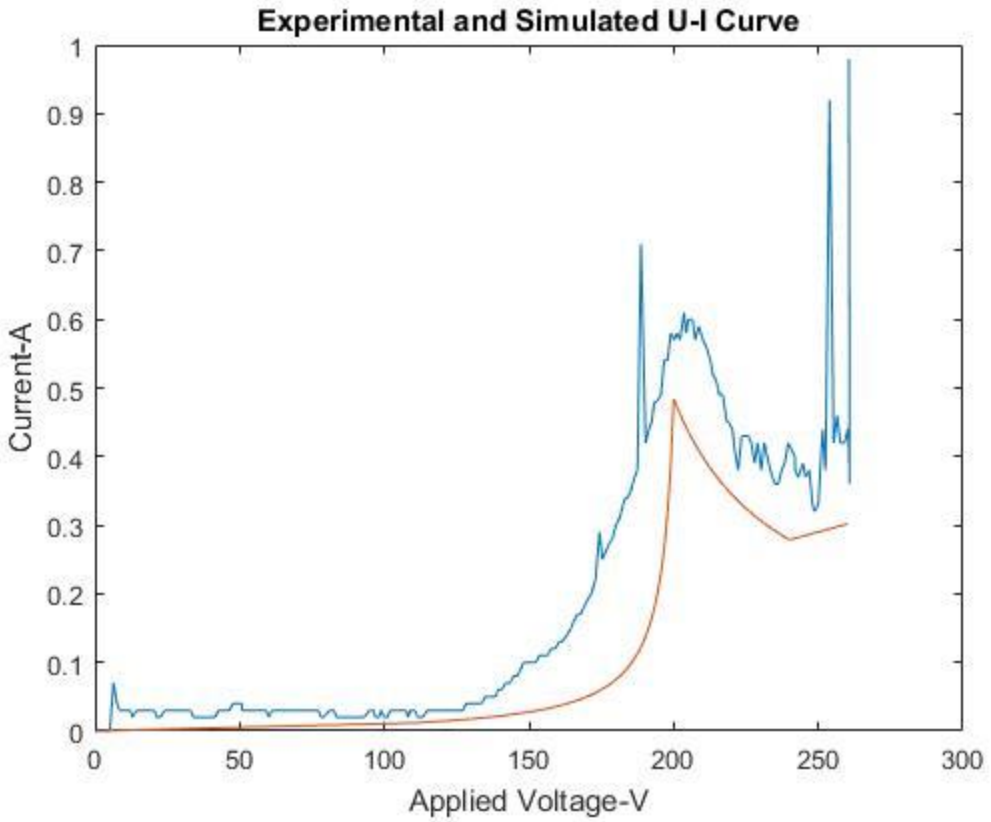


**Figure 5.3.2 (b)** Schematic of U-I curve. The conductivity of experiment is 890μΩ/cm.

Figure 5.3.3 (a) shows the voltage increases from 0 to 260.8V in 180 seconds in a liner trend, which is a very quick speed. Then, the voltage keep constant at 260.8 after that. The current increase in a liner trend slowly from 0 to approximately 0.1A at first. Then, there is a sharp increase at the end. In U-I curve showed in figure 5.3.3 (b), the whole trend is like current curve, which increase gradually like flat line before 125V. A obviously increase would be notice at around 200V. After that, a decrease to 0.4A at 240V followed by a continuously sharp increase until the end.

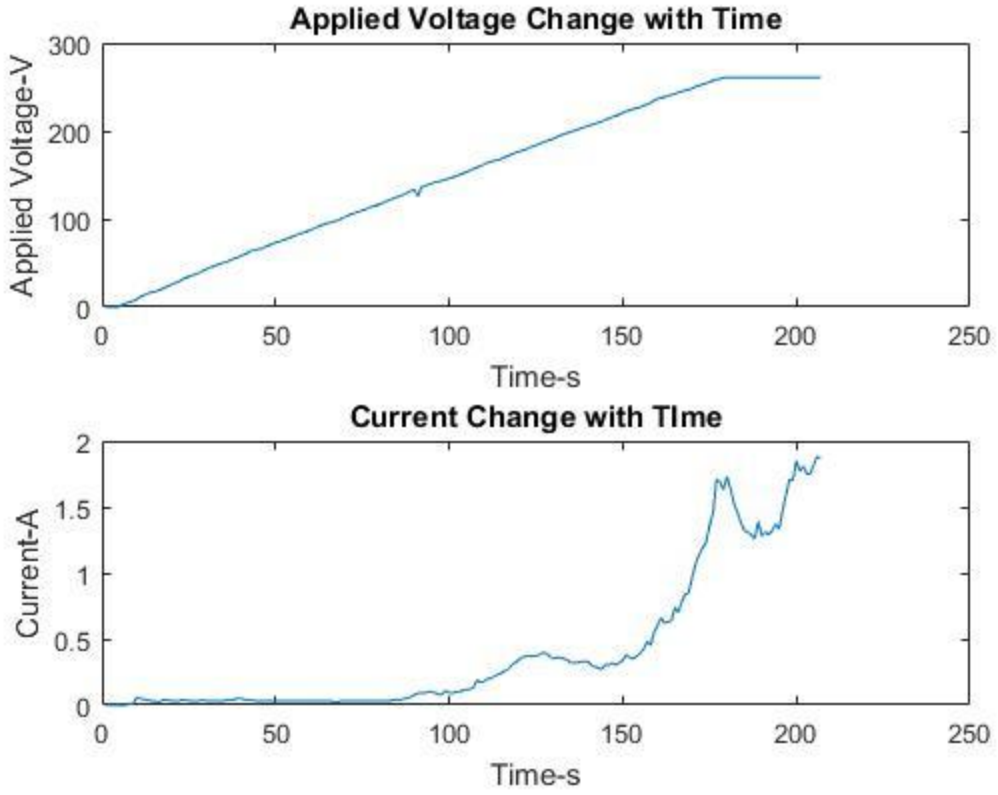


**Figure 5.3.3 (a)** Applied Voltage Change with time, Current change with time and Voltage-current curve of 1065µS/cm.

The flat slope mainly causes by constantly or slightly change total resistance of electrodes, electrolyte and passive oxidation film. Then, passive oxidation film starts dissolved at 110V and will vanished in around 200V if increasing rate in a moderate speed. After that, Resistance decrease consequently because new oxidation film formed until 240V. The slope of U-I curve represents reciprocal of resistance. Then the sharp increase follows a stable slope influence by high temperature.

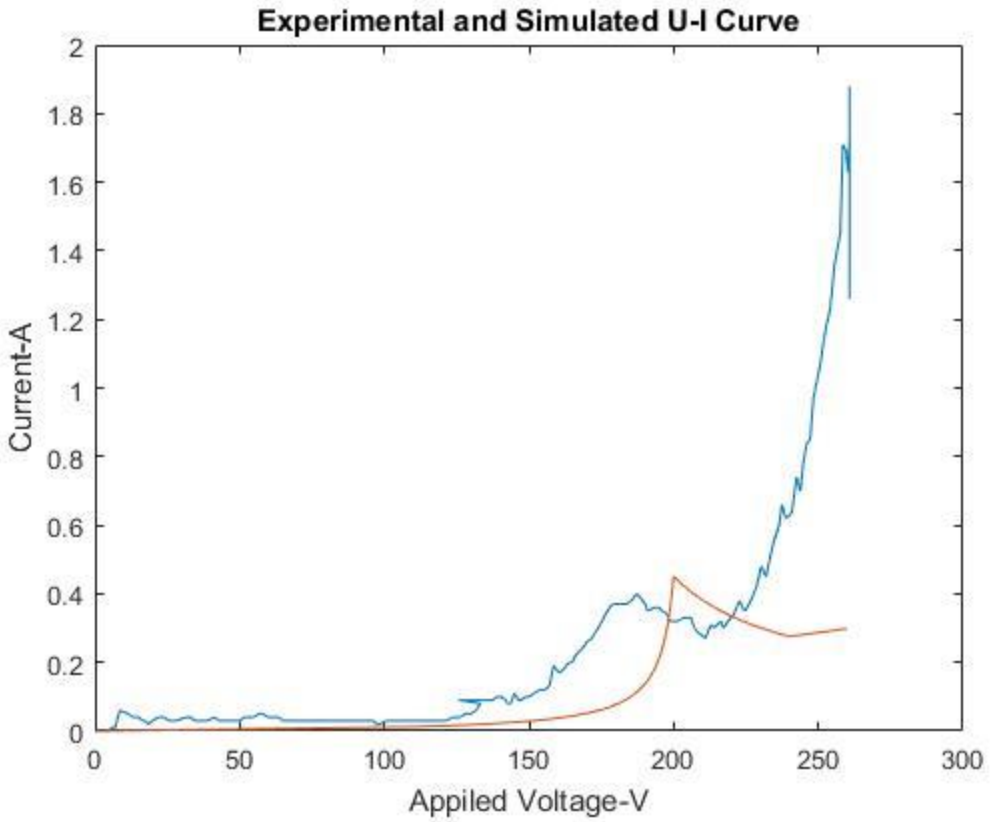


**Figure 5.3.3 (b)** Schematic of U-I curve. The conductivity of experiment is 1065μΩ/cm.

# CHAPTER 6

# CONCLUSIONS

After a series of theoretical and experimental study, we achieved a better understanding and further development of the PEO process on Ti-6Al-4V sample. 3 electrical simulated models have been built which is approximately approach to the experimental result. These models could successfully explain what exactly happened and in different phases in PEO process on Ti-6Al-4V.

Ti-6Al-4V piece was used as a sample to do all PEO experiments. Diversity results were obtained by change the conductivity of electrolyte and applied voltage. Others experimental parameters were controlled to be same as possible like surface roughness, contents of liquid solution and voltage increase speed. All the experiments were recorded by a camera then select pictures in every second. Then input the statistics in the matrix in MATLAB as the original reference, which is used to compare to the simulation result. So that the simulation model could be adjusted until it meets the experiment results. Thus, the main factors which influence resistance could be inferred. This research filled the vacancy of articles focus on PEO because it connects the theory and experiment together. In traditional research, they focus on predict what happening during each term of PEO or investigating the mechanical properties solely. This article purpose to provide an experimental exactly amount to the relationship between applied voltage and current, at the same time mentioned a theory support to the experiment researches.

The first model is a simulation before passive oxidation film starts dissolve. It has very low current because low conductivity and original passive oxidation film. Resistance of whole system almost maintain the same volume in whole progress except slightly decrease because of temperature increasing. at passive film stage, the major's resistance consists of resistance of

electrolyte and passive oxidation film of anode (Ti-6Al-4V sample). The U-I curve in this stage is nearly a straight line. While, at the new oxidation film stage, current is significant increased after flat increase because, after 110V, gradually dissolved the passive oxidation film with time. So, the U-I curve is a trend of sharp increase. Consist of resistance is decreasing resistance of electrolyte due to increasing temperature and decreasing resistance of passive oxidation film until vanish. At the arcing stage, new oxidation film will form but the resistance is quite low compare to the passive oxidation film. The resistance of the original oxidation film is 20 times higher than the new formed oxidation film. After that, the resistance become quite low because high temperature flux in electrolyte which still need to be researched because the model in this part dose not perform well.

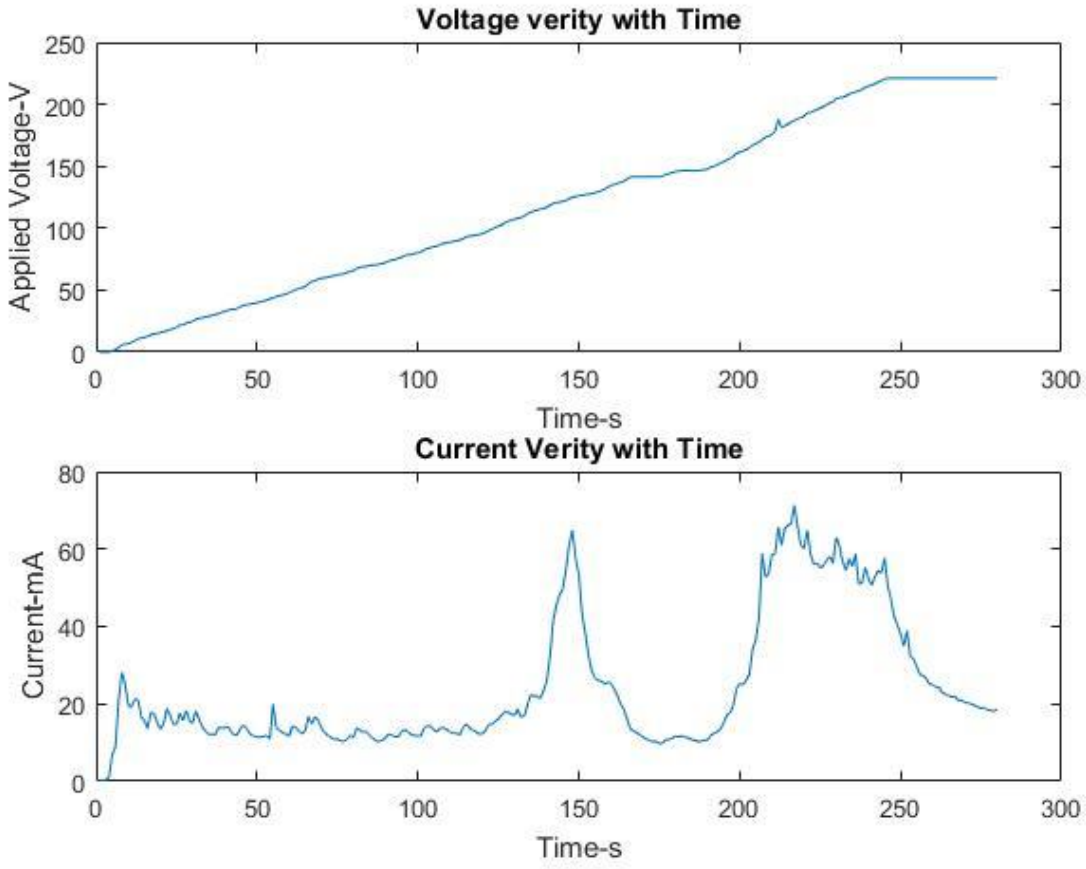


**Figure 6.1** Applied Voltage Change with time, Current change with time and Voltage-current curve of 420µS/cm. There is a interruption during flat increase of voltage.

Besides, what interesting things founded during experiments is (according to figure 6.1), after applied voltage keep constant, current will drop very fast if passive film did not start to dissolve and will keep increase flatly after passive film dissolved. This is more likely because new oxidation layer will be formed under oxidation reaction. These PEO in three stage was simulated by MATLAB models according to the majority factors analyzed. The simulation results suitable for all kind of PEO process on Ti-6Al-4V process with different conductivity but changeless surface roughness and speed of increasing applied voltage. Prediction of optimizing applied voltage is possible with this model in PEO process for Ti-6Al-4V.

# CHAPTER 7

# FUTURE WORK

Many different adaptations, tests, and experiments have been left for the future due to lack of time (i.e. the experiments with real data are usually very time consuming and boring). Future work concerns deeper analysis of plasma electrolytic deposition and its mechanic properties, new proposals to try different methods, or simply curiosity. There are some ideas that I would have liked to try during the description and the development of the fitness functions in Chapter 4. This thesis has been mainly focused on the electrical model of plasma electrolytic oxidation for simulated calculation, and most of the fitness functions used to find the best result where obtained from the literature of adapted from these or directly measured from experiment, leaving the study of fitness functions outside the scope of the thesis. The following ideas could be tested:

1) This passage only focusses on electrical model of 3 different kinds of PEO process, which corresponded to from different 3 kinds of oxidation layer in industrial use for diversity demand. The mechanic properties of the oxidation layer have not been examined in experiments. Future work should devote into investing about anti-corrosive, thermo and mechanic properties.

2) There are two kind of PED deposition, PEO and PED. And this article focuses on PEO research only. Compared with PEO process, PED process is more difficult to build electrical models because treated simple in going to be connected with cathode. Besides, bubbles and gas envelop with significantly influence current change.

3) The increasing speed of voltage is one of the most influenced factors of the beginning point of passive oxidation film formed. What we know is under medium increasing speed (1.5voltage per second), the passive film start dissolve at 110V. Fast increasing speed will force

passive film dissolve previously, but the specific volume related to increasing speed still need to be investigated.

4) Heat flux would significantly influence current trend when applied and conductivity of electrolyte is big enough especially at the end of third model, which the simulation value dose not quiet meet the experimental one. That is because electrolyte is not a homogenous solution in terms of temperature, causing accurate temperature cannot be measured be single thermometer. Thus, this part still needs to be investigated to approach experimental statistics.

Regarding the application of usage of plasma electrolytic oxidation, an extension for the near future is the use of computer-controlled DC power source in order to relief the fluctuate of current an additional task is fixing the position of two electrodes, which could let them face to face paradelle during the experiments and could exactly measure the distance between two electrodes.

## REFERENCES

[1] X. Nie, E.I. Melrtis, J.C. Jiang, A. Leyland, A.L. Yerokhin, A.Matthews. Abrasive wear/ corrosion properties and TEM analysis of $AL_2O_3$ coatings fabricated using plasma electrolysis. Surface and Coatings Technology 149(2002) 245-251.

[2] X. Nie, C. Tsotsos, A. Wilson, A.L. Yerokhin, A. Leyland, A. Matthews. Characteristics of a plasma electrolytic nitrocarburizing treatment for stainless steels. Surface and Coating Technology 139 (20)01) 135-142.

[3] A.L. Yerokhin, X. Nie, A. Leyland, A. Matthews, S.J. Dowey. Plasma electrolysis for surface engineering. Surface and Coating Technology 122 (1999) 73-93.

[4] G.I. Skanavi. Physics of Dielectricals. Strong field, Izdatelstvo Fiz. -Mat. Literatury, Moscow, 1958.

[5] Hugh O. Pierson, Handbook of carbon, graphite, diamond, and fullerenes: properties, processing, and applications, p. 61, William Andrew, 1993.

[6] Glenn Elert (ed.), "Resistivity of steel", The Physics Factbook, retrieved and archived 16 June 2011.

[7] R. M. Pashley; M. Rzechowicz; L. R. Pashley; M. J. Francis (2005). "De-Gassed Water is a Better Cleaning Agent". The Journal of Physical Chemistry B. 109 (3): 1231–8.

[8] L.A. Snezhko, L.A. Beskrovnyj, Yu.M. Nevkrytyj, V.I. Tchernenko, Zashch. Met. 16 (3) (1980) 365.

[9] L.A. Snezhko, G.V. Rozenboym, V.I. Tchernenko, Zashch. Met. 17 (5) (1981) 618, in Russian.

[14] G.A. Markov, M.K. Mironova, O.G. Potapova, Izv. AN SSSR. Ser. Neorgan. Mater. 19 (7) (1983) 1110, in Russian.

[15] A.A. Petrosyants, V.N. Malyshev, V.A. Fyedorov, G.A. Markov, Trenie Iznos 5 (2) (1984) 350, in Russian.

[16] V.N. Malyshev, S.I. Bulychev, G.A. Markov, V.A. Fyedorov, A.A. Petrosyants, V.V. Kudinov, M.H. Shorshorov, Fiz. Khim. Obrab. Mater. (1) (1985) 82, in Russian.

[17] V.A. Fyedorov, V.V. Belozerov, N.D. Velikosel'skaya, S.I. Bulychev, Fiz. Khim. Obrab. Materialov 4 (1988) 92, in Russian.

[18] V.S.Rudnev,P.S. Gordienko,preprintno.3384-B87, Inst.Khimii DVO AN SSSR, Vladivostok, 1987, in Russian.

[19] O.A. Khrisanfova, P.S. Gordienko, preprint no. 2986-B89, Inst. Khimii DVO AN SSSR, Vladivostok, 1987, in Russian.

[20] P.S. Gordienko, P.M. Nedozorov, L.M. Volkova, T.P. Yarovaya, O.A Khrisanfova, Zashch. Met. 25 (1) (1989) 125, in Russian.

[21] P. Kurze, W. Krysmann, G. Marx, Z. Wiss, Tech. Hochsch. Karl Marx Stadt 24 (1982) 139.

[22] K.H. Dittrich, W. Krysmann, P. Kurze, H.G. Schneider, Cryst. Res. Technol. 19 (1) (1984) 93.

[23] W. Krysmann, P. Kurze, K.H. Dittrich, H.G. Schneider, Cryst. Res. Technol. 19 (7) (1984) 973.

[24] P. Kurze, J. Schreckenbach, T. Schwarz, W. Krysmann, Metalloberflaeche 40 (12) (1986) 539.

[25] L.S. Saakian, A.P. Yefremov, L.Y. Ropyak, A.V. Apelfeld, Corrosion Control and Environment Protection. Informative survey, VNIIOENG, Moscow, (6), 1986, in Russian.

[26] V. A. Fyedorov, A. G. Kan, R. P. Maksutov, Surface Strengthening of Oil & Gas Trade Facilities by Micro Arc Oxidation, VNIIOENG, Moscow, (6) 1989, in Russian.

[27] G.A. Markov, B.S. Gizatullin, I.B. Rychazhkova, USSR Patent 926083, Bul. Inv. 17, 1982.

[28] L.A. Snezhko, V.I. Tchernenko, USSR Patent 973583, Bul. Inv. 23,1982.

[29] P. Kurze, W. Krysmann, G. Marx, K.H. Dittrich, DDR Patent DD-WP C25 D/236988(5).

[30] R. J. Gradkovsky, S. N. Bayles, US Patent 3956080, May 11,1974.

[31] S.D. Brown, K.J. Kuna, T.B. Van, J. Am. Ceram. Soc. 54 (8) (1971) 384.

[32] T.B. Van, S.D. Brown, G.P. Wirtz, Am. Ceram. Soc. Bull. 56 (6) (1977) 563.
[33] W. Xue, Z. Deng, Y. Lai, R. Chen, J. Am. Ceram. Soc. 81 (1998) 1365.

[34] B.R. Lazarenko, N.I. Lazarenko, Electrical Spark Treatment of Metals, Gosenergoizdat, Moscow, 1950.

[35] B.R. Lazarenko, N.I. Lazarenko, Elektron. Obrab. Mater. (1) (1966) 3, in Russian.

[36] B.R. Lazarenko, P.N. Belkin, A.A. Faktorovich, Elektron. Obrab. Mater. (6) (1975) 31, in Russian.

[37] V.N. Duradzhy, I.V. Bryantsev, Elektron. Obrab. Mater. (1) (1977) 45.

[38] V.N. Duradzhy, G.A. Fornya, Elektron. Obrab. Mater. (4) (1988) 30, in Russian.

[39] V.N. Duradzhy, A.S. Parsadanyan, Metal Heating in Electrolytic Plasma, Shtiintsa, Kishinev, 1988, in Russian.

[40] V.N. Duradzhy, N.A. Polotebnova, Elektron. Obrab. Mater. (1) (1984) 83.

[41] Linxin Zhu. Development of plasma Eelctrolytic Deposition: Princples, Process, Properties and Simulations. (2017) 1-243.

[42] Kirillov, P. L., et al. "The Look-Up Table for Heat Transfer Coefficient in Post-Dryout Region for Water Flowing in Tubes (the 1996-Version)." Preprint FEI-2525, Institute of Physics and Power Engineering, Obninsk,(Russia) (1996).

[43] Leung, L. K. H., N. Hammouda, and D. C. Groeneveld. "A look-up table for film-boiling heattransfer coefficients in tubes with vertical upward flow." Eighth international topical meeting on nuclear reactor thermal-hydraulics. 1997.

[44] Ahn, Ho Seon, et al. "Pool boiling experiments in reduced graphene oxide colloids part II–Behavior after the CHF, and boiling hysteresis." International Journal of Heat and Mass Transfer 78 (2014): 224-231.

[45] Kim, Hyungdae, et al. "On the effect of surface roughness height, wettability, and nanoporosity on Leidenfrost phenomena." Applied Physics Letters 98.8 (2011): 083121.

[46] Kim, Hyungdae, et al. "Effects of micro/nano-scale surface characteristics on the Leidenfrost point temperature of water." Journal of Thermal Science and Technology 7.3 (2012): 453-462.

[47] Berenson, P. J. "Film-boiling heat transfer from a horizontal surface." Journal of Heat Transfer 83.3 (1961): 351-356.

[48] Berenson, P. J. "Experiments on pool-boiling heat transfer." International Journal of Heat and Mass Transfer 5.10 (1962): 985-999.

[49] Tomar, G., et al. "Numerical simulation of bubble growth in film boiling using a coupled levelset and volume-of-fluid method." Physics of Fluids (1994-present) 17.11 (2005): 112103.

[50] Gerlach, D., et al. "Comparison of volume-of-fluid methods for surface tension-dominant two-phase flows." International Journal of Heat and Mass Transfer 49.3 (2006): 740-754.

[51] Tomar, G., et al. "Influence of electrical field on saturated film boiling." Physics of Fluids (1994present) 21.3 (2009): 032107.

[52] Jones, T. B., and R. C. Schaeffer. "Electrohydrodynamically coupled minimum film boiling in dielectrical liquids." AIAA Journal 14.12 (1976): 1759-1765.

[53] Nishio, Shigefumi, and Hiroyasu Ohtake. "Vapor-film-unit model and heat transfer correlation for natural-convection film boiling with wave motion under subcooled conditions." International journal of heat and mass transfer 36.10 (1993): 2541-2552.

[54] Ohtake, Hiroyasu, and Shigefumi Nishio. "Natural-Convection Film-Boiling Heat Transfer. (Experiments of Subcooled Film Boiling with Long Vapor Film)." JSME International Journal Series B 37.1 (1994): 116-122.

[55] Teh, T. H., et al. "Initial stages of plasma electrolytic oxidation of titanium."Corrosion Science 45.12 (2003): 2757-2768.

[56] Xue, Wenbin, et al. "Structure and properties characterization of ceramic coatings produced on Ti–6Al–4V alloy by microarc oxidation in aluminate solution." Materials Letters 52.6 (2002): 435-441.